UNIVERSITA' DEGLI STUDI DI MILANO

Ph.D School in Biomolecular Sciences

Scuola di Dottorato in Scienze Biologiche e Molecolari

Dottorato di Ricerca in Biologia vegetale

XXIII ciclo.

Analysis of inherent properties of Ion Channels from PBCV-1 Chlorella virus and Influenza A virus.

Tutor: Prof.ssa Anna Moroni

Tesi di Dottorato di:

Mattia Di Francesco

Matr. N° R07656

Anno Accademico 2010-2011

Contents

Introduction. 6

1) Membranes and membrane proteins. 7

2) Ion channels. 8

3) Approaches to the study of ion channels. 10

4) Potassium channels. 13

6TM potassium channels. 13

4TM potassium channels. 14

2TM potassium channels. 15

8TM potassium channels. 15

Potassium channels signature sequence. 15

5) Gating in potassium channels. 17

Voltage sensor. 17

Ball-and-chain N-terminus. 18

Bundle crossing. 19

Filter gating 20

6) Viral channels. 22

Evolution of viruses. 22

The viroporins. 23

7) PBCV-1 Kcv. 25

PBCV-1. 25

Kcv macro currents. 26

Kcv structure. 28

Kcv TM2 gating. 29

Kcv filter gating. 30

8) Influenza A virus PB1-F2. 32

Influenza A virus. 32

PB1-F2 as pathogenic factor. 33

H1N1 swine flu PB1-F2. 34

PBCV-1 Kcv. 35

Materials and Methods. 36

1) Xenopus laevis Oocytes preparation for electrophysiological measurements. 37

2) Electrophysiology. 38

3) Evaluation of fast gating. 39

4) Determination of the apparent single-channel current, Iapp. 39

5) Determination of the true single-channel current, Itrue, and of the rate constants of an O-C model of fast gating. 40

Results. 41

Fast Gating. 46

Slow gating. 55

Applications. 57

Discussion. 58

Fast Gating. 60

Slow gating. 62

Applications. 64

Influenza A PB1-F2. 66

Materials and Methods. 67

1) In vitro protein production. 68

2) Protein reconstitution and electrophysiological measurements. 68

3) Cell culture and macro currents measurements. 69

4) Microfluorimeter essay. 70

Results. 71

Reconstitution of aPB1-F2sf in planar Lipid bilayers. 74

Macroscopic membrane currents. 76

Fluorescence Microscopy. 85
Model. 88
Discussion. 90
Single-channel characterization of aPB1-F2sf in artificial lipid bilayer. 92
PB1-F2 generates an elevated conductance in mammalian cells plasma membrane. 93
Possible role of PB1-F2 in Influenza A infection cycle. 95
Conclusions. 97
References. 99
Dedicato a… 109

Introduction

1) Membranes and membrane proteins

Cells are surrounded by an external envelope, known as plasmalemma, external, or cell membrane, that separates the interior of the cell from the external environment. This structure regulates the uptake of nutrients from the external environment, the release of molecules from the cell, and has a key role in the communication with other cells, or in sensing environmental conditions.

A lipid membrane can be crossed just by small molecules like water or gas, or by non-charged molecules. Therefore, the role of membrane proteins involved in the transport of molecules is important for the physiology of cells. In this group we can distinguish between active and passive transporters.

Active transporters are proteins that move molecules or ions against their electrochemical gradient. This mechanism requires energy. In the case of ATPases, it is normally supplied by ATP hydrolysis. In the case for example of the bacterial Rhodopsin, photons provide the energy. This is called primary active transport, whereas in secondary active transport the energy is provided by the coupling with the transport of another ion that migrates downhill along its gradient. This coupled transport (or cotransport) can be divided in symport, when the transported and the coupled molecules migrate in the same direction, and antiport, when the two molecules moves in the opposite direction.

On the contrary, passive transporters regulate the selective movement of one or a small group of molecules towards their electrochemical gradient (uniporters). We can find in this group carrier proteins and ion channels. Carriers regulate the passage of big molecules across the membrane, like for example GLUT transporters, responsible of the internalization of Glucose in the cell. Ion channels characteristics will be discussed in the next chapter.

Lipid membranes don't have the only function of external cell envelopes, they surround in fact also internal cell compartments, like the nuclear, mitochondrial, Liposome, or Vacuole membrane. Also here they regulate the passage of molecules, modulating the organelle activity, and resulting for example in a different gene expression.

2) Ion channels

Ion channels are proteins that regulate the selective passage of one or few ionic species across the membrane, downwards their electrochemical gradient.

The different ionic concentrations generated by the active transport, generates a chemical and electrical gradient across the membrane. When ion channels are in an open conformation, ions can cross the membrane following these gradients: the chemical gradient tends to equilibrate the osmotic difference by moving ions towards the solution with the lower concentration; while the membrane potential generates an electrical gradient, that force ions to move towards the side with opposite charge. The majority of the cells accumulate, under resting conditions, negative charges at the cytosolic side. This corresponds to a negative value of the membrane potential. The electrochemical gradient would be rapidly dissipated by the action of channels, if active transporter were deleted.

Ion channels are present in any kind of cell, where they execute many function important for its physiology. Changes in the value of the membrane potential is a signal that can ether induce changes in the cell metabolism, ether be transmitted to the other surrounding cells. For example ion channels in neurons in neurons generate the action potential, and enable its transmission along the axon by the presence of manly Na^+ and K^+ voltage-gated channels. Taste buds are rich in receptor cells, where many TRP (Transient Receptor Potential) channels are present. TRP channels generate an action potential after the interaction with specific molecules, and are responsible for the sensitivity to many environmental stimuli.

Physiological mechanisms can be controlled also by ion channels located in the membrane of internal compartments. Ca^{2+}-induced Ca^{2+}-release is a cell signal that coordinates processes such as muscle contraction, neurotransmitter release in nerve cells, or release of hormones in endocrine cells. This mechanism is based on a release of Calcium ions from the ER to the Cytosol as induced by a small increase of cytosolic Ca^{2+} concentration, that opens Ca^{2+}-dependent Ca^{2+} channels.

Ion channels represent a big group of proteins that had been classified on the basis of many characteristics; two main parameters are used to describe channels properties: selectivity and gating.

The selectivity is the ability of a channel to discriminate between ions by means of the polarity or the strength of their charge, or their electronic density, and therefore select the passage of one or a small group of ions. We can find for example channels extremely selective for one only ion (selective channels); channels that allow the passage of many different positively charged ions (cation channels); or channels that allow the passage of a large group of ions, even if with different polarity or charge strength (non-selective channels).

Selective and non-selective channels differ a lot in their function and structure: selective channels are normally composed by a complex of α-helix that cross the membrane and interact in order to form an

hydrophilic pore region where ions can pass through. They often present a domain at the cytosolic or external side that, interacting with other molecules or with other proteins, confer to the channel a receptor behavior: these interactions result indeed in a regulated activity of the channel. In some channels , the selectivity for one ion is due to the presence of a selective filter region, as described below for K^+ channels.

Non-selective channels can be composed by a variable number of single α-helix transmembrane subunits that interact forming a central pore region. The number of subunits that cooperate to form the channel can affect its selectivity and its conductance. These channels normally behave like simple pores, and are not linked to any domain sensitive to environmental stimuli.

Another characteristic important for the classification of ion channels is the gating. Gating is the property of a channel to randomly switch between an open and a close conformation, allowing or denying the passage of ions. Many factors can induce such a conformational change, and different mechanism can be the origin of opening/closure events. A well known gating mechanism is that of voltage dependent Na^+ K^+ and Ca^{2+}channels: the fourth of six transmembrane domains (S4) is rich in positive charges. When the membrane potential shifts to more positive values (depolarization), the positive charges accumulated in the intracellular side induce the voltage sensor S4 to move towards the extracellular side, resulting in an activation of the channel. Other gating mechanisms have been described in many channels, also concerning the movement of other domains: for example it has been shown that conformational changes of the slide helix in Kir channels (Inward Rectifier K^+ channels) is transmitted to the Filter region, and modulate the opening of the pore (W. Zhou and L. Jan; 2010). A more detailed description of these mechanism related to conformational changes is presented in the chapter “Gating in potassium channels”.

Mutations in the sequence encoding for ion channels can lead to a change in gating properties. This is the case of channelopathies: a mutated ion channel leads to an altered or not functional cell mechanism, and consequently a disease. Many forms of epilepsy have been found to have a genetic origin, where the mutation of an ion channel encoding sequence is responsible of an affected neuronal behavior. In the case of Juvenile myoclonic epilepsy, the mutation G715E in the gene *Clcn2*, encoding a chloride channel highly expressed in brain neurons, results in an altered voltage dependence: for this mutant, activation occurs at more positive potentials compared with the wt channel, causing an increased neuronal excitably.

3) Approaches to the study of ion channels

The study of ion channels behavior, and the diseases related to their abnormalities had been of growing interest in the last decades, and many technique have been developed for an always more detailed analysis of their characteristics. Two main approaches are used in the laboratory where I have been working during the PhD: crystallography and electrophysiology.

Crystallography is a technique that allow to define the three-dimensional structure of a protein: a crystal is obtained under determinate conditions, that can vary from protein to protein, and is irradiated with high purity and high intensity X-rays, generating a diffraction pattern. Applying the Fourier transformation to the diffraction pattern data, in some cases it becomes possible in some cases to reconstruct the tridimensional structure of the studied protein. The resolution can be very high, normally in the range of a few Angstrom. Thus, information on the position of atoms and their interactions can be obtained.

Electrophysiology deals with the study of currents generated by functional ion channels inserted in a membrane. Heterologous expression system are used for in-vivo synthesis of channels, as *Xenopus laevis* oocytes or mammalian cells, and ionic currents can be measured by the usage of microelectrodes by means of two main system: Two Electrode Voltage-Clamp (TE Voltage-Clamp) and Patch-Clamp.

TE Voltage-Clamp measurements are performed by inserting two microelectrodes into a cell, and imposing a fixed membrane potential: one electrode measures membrane potential and the other one injects a current. This current is controlled by a feed-back loop that regulates the injected current in such a way that the measured membrane potential becomes equal to the command potential. That potential is selected by the operator and given to the feed-back amplifier as a set-point. With this technique it is possible to quantify the ionic current passing through all the channels present in the cell membrane. In the vicinity of the reversal potential V_{rev} the current-voltage relationship often can be described by Ohm's law:

$$V - V_{rev} = I \cdot R \qquad \text{Eq. 1}$$

With R = constant being the slope resistance of the ion channel IV-curve at that potential. V is the clamped potential, V_{rev} is the reversal potential (the value of membrane potential where no net flux of current is measured), I is the measured current, and R is the ion channels resistance. Eq. 1 describes a local linearity. However, most channels are non-linear, and R is replaced by a differential quotient dV/dI which depends on the actual membrane potential.

We can use as parameter the ion channels conductance G, that corresponds to the reverse of resistance (G = 1/R). For linear sections of the current-voltage relationship we can describe therefore the measured

current as:

$$I = (V - V_{rev}) \cdot G \qquad \text{Eq. 2}$$

If we consider to have N channels in the membrane, G will correspond to the conductance of all N channels, that are characterized by a single-channel conductance g, and a single channel open probability p. The equation becomes:

$$I = (V - V_{rev}) \cdot N \cdot g \cdot p \qquad \text{Eq. 3}$$

Currents generated by all the channels inserted in the cell membrane are considered as macro-currents. The determination of single channel parameters requires the usage of the Patch-Clamp technique.

Patch-Clamp measurements are performed using a single electrode that, at the same time, clamps the membrane potential, and measures the current given to the system in order to fix the voltage value. In order to isolate a small area of the membrane, a seal is obtained with the glass electrode: when the tip of the micropipette gets in contact with the cell membrane, a negative pressure is applied in order to such a small area of the membrane. This pressure is applied until the formation of a seal that isolates the electrical flow through the membrane area (Patch) from that of the rest of the cell. Thus it is possible to measure currents generated by the activity of only those ion channels which present in the Patch. If only one or a few channels are in the membrane of the patch it becomes possible to measure single ion channels fluctuations. This technique, renovating the study of ion channels properties by enabling a detailed analysis of their functions, was valid for the assignation in the 1991 of the Nobel Prize in Physiology or Medicine to Erwin Neher and Bert Sakmann (Neher E. and Sakmann B., 1976; Neher E., Sakmann B. and Steinbach J.H., 1978).

The Patch-Clamp technique allows to record ion channel activity in different configurations: Cell-Attached, Whole-Cell, Outside-Out and Inside-Out.

In the Cell-Attached configuration, the glass electrode remains on the cell; the internal and external of the Patch correspond to the cytosolic and pipette solutions respectively. In order to pass from Cell-Attached to Whole-Cell configuration, the membrane of the Patch is broken by a current pulse, or by a strong negative pressure. In this configuration the current activity of the ion channels inserted in the whole cell membrane is recorded. It is possible to pass from the Cell-Attached to the Outside-Out configuration by slowly drawing the glass electrode from the cell surface. When it is pulled, the portion of the membrane that surround the

tip of the electrode tends to close leaving the external side directed to the bath solution and cytosolic side directed to the pipette solution. In order to pass from the Cell-Attached to the Inside-Out configuration the electrode is rapidly pulled out from the cell surface. In this way, the cytosolic side of the ion channels inserted in the Patch is exposed to the bath solution, that can be easily changed in order to test the effect of a different cytosolic environments on the channel activity. Thus, changing such a solution, the effect of a different cytosolic environments on the channel activity can be easily tested.

The knowledge obtained by crystallographic and electrophysiological techniques can be put together resulting in a detailed and complete structure-function description mechanisms of ion channels.

4) Potassium channels

Potassium selective ion channels control and regulate a multitude of the cell physiological functions. This is indeed one of the best studied group of channels, and many characteristics of their behavior have been described.

Potassium channels can be divided on the basis of the number of transmembrane domains (TM) that compose the single subunit: we can find indeed 2TM, 4TM, 6TM, and 8TM K^+ channels (Fig. 1).

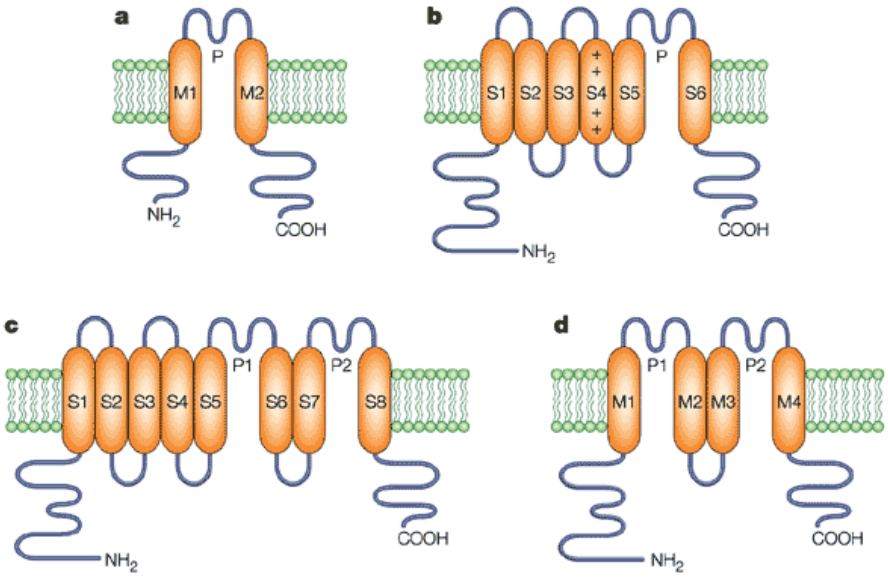

Fig 1: Schematic representation of the structure of 2TM (a), 6TM (b), 8TM (c), and 4TM (d) potassium channels.

6TM potassium channels.

The group of 6TM K^+ channels include Voltage-gated (Kv), and Ca^{2+}-activated (K_{Ca}) potassium channels. Four α subunits assemble to form homotetrameric channels, when the subunits are identical, or heterotetrameric channels, when the subunits are different. These channels present two cytosolic domains at the N- and C- terminus, and a small loop, called P, between TM5 and TM6. The tetramerization of the α subunits arranges the four P loops in order to build the Filter region of the channel. The fourth transmembrane domain (TM4) is characterized by the presence of positively charged amino acids, that are responsible of the sensitivity to voltage changes as found in Kv channels. The possibility to change conformation, and thus opening or closing in response to the membrane potential is an important characteristic of Kv channels, crucial for a multitude of biological signals such as the initiation and the

propagation of action potentials in neurons.

In the physiology of a cell, the cytosolic concentration of calcium ions is an important parameter that, when modulated, can initiate a cascade of events leading to huge changes of the cell behavior. K_{Ca} channels are activated by intracellular calcium, and therefore transduct these signals regulating many cell mechanisms. This group of channels is divided into BK, IK and SK, on the base of their conductance (Big, Intermediate and Small K^+ conductance); the three types are also different in voltage dependence, Ca^{2+} sensitivity and pharmacology (they are blocked by different toxins). K_{Ca} channel α subunits are composed by six transmembrane segments, with the exception of BK channels, where another transmembrane domain (TM0) was found at the N-terminus, which ends at the external side of the membrane. The sensitivity for Ca^{2+} ions is mediated in these channels by a cytosolic domain at the C-terminus domain, where negative charges directly bind calcium. This domain is in fact considered as an inhibitor of voltage-depend channel opening whose negative effect are relieved by calcium.

Different proteins often aggregate in complexes in order to cooperate and modulate their activity; also ion channels interact with other transmembrane proteins with the same goal. The activity of 6TM K^+ channels can be modulated by β subunits, auxiliary proteins able to associate with α subunits and modify the channel's voltage dependence, its gating mechanism, or other channel properties. The β subunit interacting with potassium channels that was firstly described is MinK (encoded by the gene KCNE1): the potassium channel KCNQ1 was found to have a small current in comparison with other cardiac outward rectifier potassium channel; its cotransfection together with KCNE1 was able to increase currents tenfold and slow the activation kinetics. Other β subunits can have an inhibitory effect: Kv1.5 display a small inactivation when steps of voltages from -100mV to +50mV are given; when cotransfected with Kvβ1 the inactivation kinetic increases dramatically. The N-terminus sequence of Kvβ1 was found to be similar to the “ball domain” that characterize the inactivation gating of Shaker potassium channels (see chapter “Gating in potassium channels”).

4TM potassium channels.

Searches of new genes revealed the presence of sequences encoding subunits of potassium channels with two P loops: P1 and P2, surrounded respectively by the transmembrane domains TM1-TM2 and TM3-TM4. These potassium channels, composed of four transmembrane domains, are known indeed as tandem-pore-domain potassium channels, and their functional structure is given by the association of two α subunits. 4TM potassium channels are responsible for the so called “leak currents”, and the regulation of the cell excitably. Their activity can be regulated by many factors such as pH, mechanical stress, oxygen tension, or interaction with second messengers. For example, the 4TM potassium channel TASK-1 can be open by volatile anesthetics, resulting in a hyperpolarization of neuronal membranes and a consequent depressed

brain activity.

2TM potassium channels.

The class of channels with two transmembrane domains is composed by the smallest potassium channels known so far; hence they are interesting for the understanding of mechanisms related to the central core of this group of membrane proteins. They are indeed composed by the pore unit of potassium channels, corresponding to TM1, TM2, a P loop, and, in some cases, cytosolic N- or C- terminus domains. Ion channels arise from the association of four α subunits, that can assemble to form homo- or hetero- tetramers. The study of 2TM potassium channels properties begun with the analysis of the so called "K^+ inward rectifier" channels (K_{ir}), that display a voltage dependence which enables inward currents only. A blocking mechanism was found to be responsible of such a behavior: intracellular Mg^{2+} and polyamines, such as spermine, spermidine or putrescine, are able to enter the channel, and block the movement of K^+ ions towards to the extracellular solution. The measurement of K_{ir} currents in Inside-Out configuration demonstrated that the rectification of the outward currents can be removed when any possible channel blocker is eliminated from the intracellular solution. The strong voltage dependence of K_{ir} channels is an important characteristic that reduces the dissipation of K^+ electrochemical gradient during the cardiac action potentials of heart cells.

8TM potassium channels.

More rare is the case of potassium channels composed by subunits of eight transmembrane domains. For example, in the genome of Yeast the 8TM potassium channel TOK was identified. This is another case of tandem-pore-domain potassium channel, composed by a 6TM module attached to a 2TM one; like 4TM channels, the functional protein is formed by the assembly of two α subunits.

Potassium channels signature sequence.

Among all potassium channels, the sequence encoding the filter region (-TXXTXGY/FG-) is highly conserved, and the generated structure is at the basis for the selectivity for K^+ ions. This sequence represents the finger print of this group of membrane proteins, hence it has been called "potassium channel signature sequence". The filter structure arising from the association of α subunits was determined at atomic resolution (2 Å), with the crystallization of the 2TM potassium channel KcsA, and the important knowledge coming from its analysis was valid for the awarding in the 2003 of the Nobel Prize for Chemistry to Roderick McKinnon. Four potassium ion binding sites were found in KcsA filter, coordinated by five oxygen: four carboxyl oxygen coming from the backbone, and one from a threonine residue. This kind of structure

simulates the electrostatic environment that surrounds ions in water solution, and is responsible for the high conduction rate that characterize potassium selective channels: ions are not subjected to any environmental electrostatic change passing from the solution to the interior of the channel.

The four potassium binding sites cannot be occupied simultaneously: electrostatic forces would repulse ions lying in two adjacent sites. Only two potassium ions can be found in the filter at the same time, alternated by two water molecules: the two possible configurations results from the occupancy by potassium ions of the first and the third binding sites (configuration 1, 3) or the second and the fourth sites (configuration 2, 4) (Fig. 2).

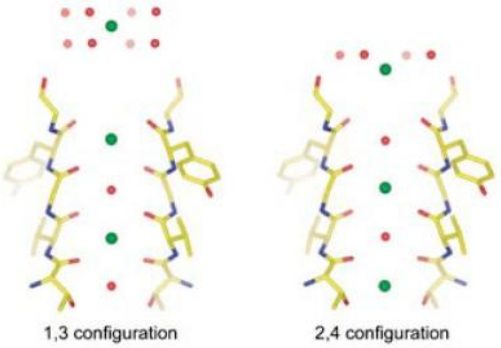

Fig. 2: Crystal structure of KcsA potassium channel Filter region with potassium ions (green dots) and water molecules (red dots). The four binding sites can be occupied with two distinct configurations: configuration 1, 3 (left) or configuration 2, 4 (right) (McKinnon et al., 2001).

The described structure of the domains composing a potassium channel is not rigid: interactions established between atoms belonging to the same protein, or with environmental molecules, or environmental stimuli, lead to conformational changes that can be reflected in a different channel behavior. Some of these changes can be responsible for the modulation of the ion conduction pathway, generating the so called “gating mechanisms”.

5) Gating in potassium channels

As already discussed in chapter 2 ("Ion Channels"), the gating is the property of a channel to fluctuate between an open and a close conformation, allowing or denying the passage of ions. Such a mechanism implies a conformational change, and can be induced by a multitude of factors, like the interaction with substrates or with other subunits, or environmental changes (voltage, pH, temperature, light, ecc). The biological evolution differentiated channels on the base of the selectivity for specific ions. However, many of the gating mechanisms described in this chapter have similar features even among channels belonging to different groups, leading to hypothesize a possible common origin.

Gating mechanisms are usually described with an "open to close diagram", characterized by rate constants ($k_{close \rightarrow open}$ and $k_{open \rightarrow close}$) indicating the rate of passage from one state to the other. A more detailed analysis demonstrate that channels may be characterized by more than one open or closed state, or by activated, inactivated, deactivated or blocked states; the open to close diagram becomes than more complex when all the possible channel states have to be described.

Voltage sensor

An important gating mechanism described for potassium channels is that one which confers sensitivity to changes of the membrane voltage. In order to induce a conformational change in response to changes in membrane potential, the movement of charges belonging to the channel or interacting with it is necessary. Investigating on the presence of charged amino acids, a conserved sequence was found in many sodium, calcium and potassium channels: in 6TM potassium channels, the sequence belongs to the fourth transmembrane domain (S4), and is characterized by the presence of five to seven positive amino acids, separated each by two neutral amino acids. S4 is an α helix that makes a complete turn every 3,6 amino acids, and the position of the positive residues results in a charged stripe surrounding the transmembrane domain (Fig. 3).

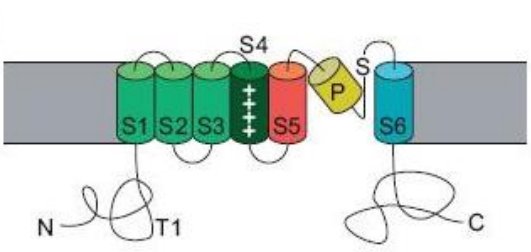

Fig. 3: Schematic representation of 6TM potassium channels. The voltage sensor (S4) presents positive charges.

During hyperpolarization S4 is attracted by the internal negative charges, and its position is directed to the cytosolic side of the membrane. Once the voltage depolarizes, S4 is shifted towards the extracellular side,

generating a conformational change that result in the final opening of the channel. The movement of potassium ions from the cytosol to the external solution repolarize the membrane potential, shift S4 towards the internal side, and close again the voltage-dependent potassium channel. Mutation in the S4 sequence, leading to the deletion of the positive charges, results in a progressive reduction of the steepness of the depolarization-induced activation, and its shift to more positive potentials, demonstrating in that way the key role of the charged amino acids (Cannon S.C., 2010).

The movement of gating portions of ion channels can be studied also by the measurement of the so called "Gating Currents" (I_g), generated by the charged amino acids of the S4 domain after changing the membrane voltage. These currents are smaller in comparison to those generated by ionic flux through the same channel, and the usage of blockers or low permeable ions, or a mutant which does not conduct current, is necessary for such a measurement. Gating currents are generated by the movement of "Q_{on}" charges when the channel is activated, and "Q_{off}" charges when the gate closes, and their kinetics are related with the velocity of the S4 movement: potassium channels, that activate more slowly than sodium channels, display smaller gating currents. S4 movements can be detected also when the channel, without opening, passes among different close states

Ball-and-chain N-terminus

Another gating mechanism has been widely studied in sodium channels and Kv Shaker potassium channels, and explained with the traditional "Ball-and-Chain" model (Armstrong C.M. and Bezanilla F., 1973). Shaker potassium channel are responsible for repolarization of neuronal cell membranes, after the fast depolarization phase induced by the opening of Na^+ voltage gated channels. They are known as delayed-rectifier K^+ channels on the base of their deferred opening, during the action potential, compared to Na^+ channels. Like the other Kv channels, they open the activation gate as response to depolarization, and, after a time that can be different for each channel, another gating mechanism inactivates the ion passage, in the same condition of depolarizing membrane potential. This block was found to have similar characteristic to that described for cytosolic quaternary ammonium (QA) ions like TEA, and was demonstrated to be induced by the entrance of the cytosolic N-terminus domain in the internal mouth of the channel: the depolarizing potential tends to move this domain, that is positively charged, from the Cytosol in the direction of the external solution, where negative charges are accumulated; the "ball" domain, when enters in the cytosolic mouth of the channel, obstructs the passage of ions (Fig. 4). Experiments on the ShB variant of Shaker potassium channel demonstrated that deleting the first 22 amino acids in the N-terminus (the "ball" domain), the inactivation gate is removed, and that modifying the length of the amino acids from 23 to 83 (the "chain" domain) the rate of block from the ball domain is modulated. The block is than removed by inward K^+ currents at hyperpolarization voltages.

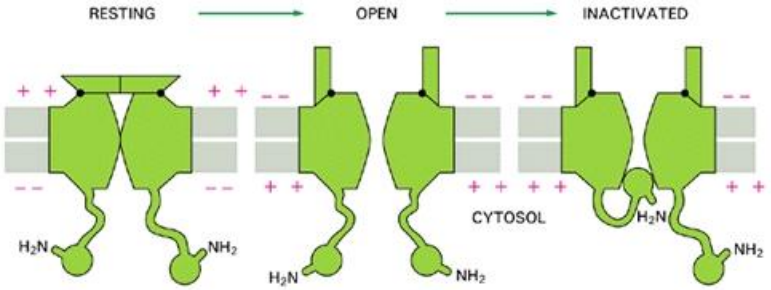

Fig. 4: N-type inactivation. The ion channel can pass from a closed (left) to an open (center), and an inactivated (right) conformation.

Bundle crossing

The comparison of crystal structures from two different potassium channels was important in the finding of the "Bundle Crossing" gating mechanism. KcsA, the first 2TM potassium channel crystallized, was found to cross the C-terminal portion of the second transmembrane domain, highly reducing the side of the cavity directed to the cytosolic solution (Perozo E., Cortes D.M., Cuello L.G. 1999). On the contrary, MthK, another 2TM potassium channel, cloned from *Methanobacterium thermoautotrophicum*, was crystallized in the open conformation. The main difference with the KcsA crystal is that the last amino acids of the second transmembrane domain display a 30° rotation starting at the level the Glycine 83; wile in KcsA, at the level of the corresponding Glycine (G99), no rotation is appreciable. This Glycine, at the basis of the bundle crossing gating mechanism, was found to be conserved in many potassium channels (Fig. 5).

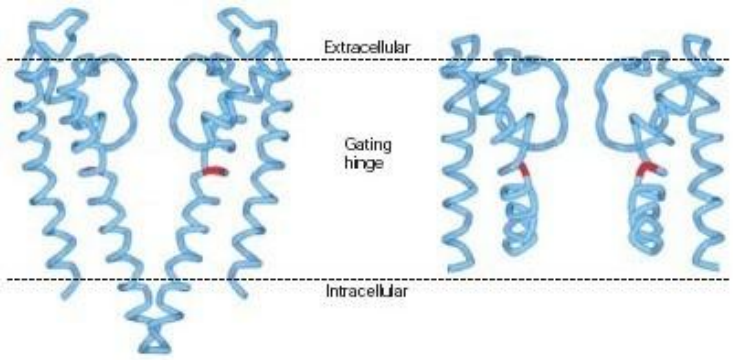

Fig 5: Crystal structures of KcsA (left), crystallized in the close conformation at the bundle crossing level, and MthK (right) crystallized in the open conformation. For both channels, the Glycine knee is highlighted in red.

Filter gating

Even removing any kind of possible channel blocker from the internal solution, some potassium channels were found to be affected by a slow current decrease, named “C-type inactivation” in contrast with the faster “N-type inactivation” generated by the Ball-and-Chain N-terminus domain of Shaker potassium channels. The comparison of fluorescence spectroscopy (Blunck et al., 2006), EPR and electrophysiological measurements (Cordero-Morales et al., 2006) gave the idea that KcsA could enter in an inactivated state even when the bundle crossing gate was open, and it became of growing interest the understanding of which portion of the channel could be involved in the C-type inactivation.

Already in the latest 70s, hypothesis on the role of the filter region was elaborated in order to explain the “anomalous mole-fraction behavior” (Hagiwara S., et al. 1977), which consist in the modulation of the conductance level resulting by the different ions that permeate the channel. It was then demonstrated that also the kinetics of the C-type inactivation can be affected by different permeating ions, stressing on the idea that the filter region, despite its potassium ion coordinating structure, considered to be rigid, can be affected by gating mechanisms.

A definitive demonstration of the control of the channel conductance by the filter region was given by mutating KcsA at the level of the filter helix, the domain lying just behind the filter amino acids (Cordero-Morales et al., 2007). This region was found to directly interact with the filter, controlling its rigidity by promoting or disrupting salt bridges. A key role is played by the glutamic acid at position 71: mutating this amino acid in alanine, its interaction with the aspartate at position 80 is deleted, resulting in a strong increase of the single channel open probability, without affecting its unitary conductance. The C-type inactivation was then described as a reorientation of the filter backbone, leading to a gradual loss of the second and the third potassium binding domain (S2 and S3, from the external side) abrogating the ion conduction.

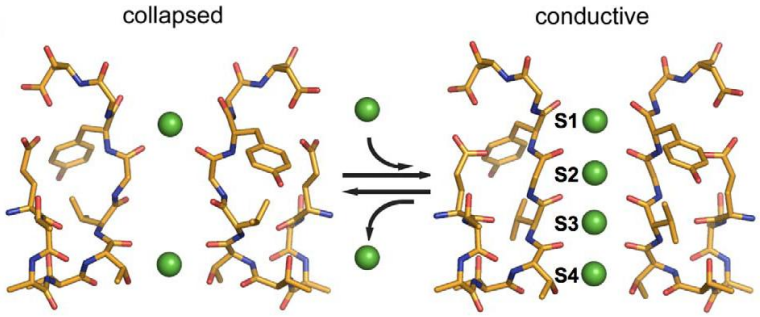

Fig. 6: KcsA filter structures in the collapsed (left) and conductive (right) conformations (Lockless S.W., Zhou M., MacKinnon R, 2007).

Crystal structures in different ionic conditions demonstrated that the stability of the filter can be controlled also by the permeating ion concentration: the filter of KcsA was found to maintain a conductive conformation with high potassium (200mM KCl), but enter in a collapsed state at low potassium concentration (3mM KCl) (Lockless S.W., Zhou M., MacKinnon R, 2007) (Fig. 6). This finding is in agreement with the Ion Depletion Model (Schroeder I. and Hansen U.P., 2007; Abenavoli A., et al., 2009), that consist in temporary and fast closure events at extreme membrane potentials, contrastable by an increased potassium concentration (see Results, PBCV-1 Kcv, Fast gating).

The unitary conductance of some ion channels was found to increase or decrease in discrete steps, generating the so called "Subconductance levels". Such a phenomena is interpreted as resulting from a transition between different open states, that can be induced, as described for $GABA_A$ and glycine receptors, by the interaction or the dissociation of substrates molecules with single α-subunits of the conducting channel. The same behavior was found in Shaker potassium channels, where the subconductance levels differed in ion selectivity, as if representing rearrangements of the selectivity filter (Zheng and Sigworth, 1997, 1998).

It has been lastly shown that also rearrangements of the cytoplasmic domain can be transmitted to the filter region of Kir channels, resulting in a modulation of its structure, and the transition from a conducting to a blocked or non-conductive state (Clarke O.B., et al., 2010).

All together this knowledge gives an idea of a potassium filter region far from a rigid structure, that, at the contrary, must be flexible in order to adapt to the surrounding conditions, or control the ion conduction rate, and thereby is central in the modulation of important physiological mechanisms.

6) Viral channels

Evolution of viruses

Viruses are genetic molecules, transported by a proteinic envelope, that necessitate to infect an host cell and use its replication and expression machinery in order to duplicate their genome and synthesize viral proteins. For this reason they are not considered as living cells, but as mobile genetic elements like Plasmids or Transposons.

The evolutionary collocation of viruses is not yet clear, and different theories had been proposed describing their origin: some of them describe viruses as originating from cells, while other theories separate their evolution. The *regressive theory* propose that symbiotic bacteria progressively lost some of their genes, and the relative capabilities. They could be replaced by the host cell, thus rending the symbiotic organism incapable to replicate independently, and therefore transforming it to a virus (Lustig A, Levine AJ., 1992). On the other hand, the horizontal genetic transmission that characterize viruses, together with the similarity of proteins encoded by organisms that do not seem to have a common ancestor, could indicate a possible role of viruses in the transmission of nucleic acid sequences between different cell species. The study of bacterial T4 phages and large DNA eukaryotic viruses such as phycodnaviruses (infecting microalgae) opened the door to the suggestive theory that describes eukaryotes as resulting from the viral infection of a prokaryotic cell, that progressively transformed the viral DNA and its lipid membrane into the cell nucleus (L.P. Villarreal and V.R. DeFilippis, 2000). Another theory that correlate cells and viruses hypothesize that the genome of a cell could have gained an independent self replicating property, becoming a viral particle.

On the contrary, the *co-evolution theory* separate the viral and the cell evolution, proposing instead a common origin for virus, plasmids and transposons, which share similar characteristics. However, the recent study of Mimivirus, an unusually big size (750nm) and large DNA (1,2Mb) quasi-autonomous virus, is changing the discussed theories: this is for example the first virus found to encode enzymes involved in the protein translation machinery, suggesting a vertical evolutionary origin of cells and viruses from a common ancestor (J.M. Claverie and C. Abergel, 2010).

The viroporins

What is commonly accepted is the ability of viruses to reduce the protein size, and minimize their genome. Their study revealed indeed unexpected strategies to compact genetic molecules, different from those of all other known organisms. For example some viruses, like hepadnavirus or Influenza A virus, are able to encode different proteins starting from the same nucleotide sequence. For this issue they can shift the reading of the same mRNA molecule (frameshift or alternative open reading frame), or employ different mRNA splicing to maximize the number of proteins that can be synthesized.

Once an organism is infected by a virus, it produces a high quantity of antibodies, molecules able to recognize the proteins on the viral envelope surface, inducing the immune system response and the consequent viral particle degradation. In order to bypass the antibody recognition, viruses can change the structure of their proteins by "antigenic drift" or "antigenic shift": the first consists in a mutation of a gene already present in the viral genome, and allow the infection of an organism that had already been infected before the mutation; the second is a substitution of a viral gene with a new one; introducing a new sequence in the viral genome, it is possible for a virus to infect again the same population. Changes in the viral genome can be triggered when a virus passes from an endemic to an epidemic or pandemic state: the higher propagation velocity increases the viral genetic pool, introducing new proteins that, lying not only on the external envelope, can improve the viral pathogenicity.

Viroporins are viral proteins able to homo-oligomerize in the host membrane thus forming ion channels. In many cases they result to be essential in the development of the viral cycle, and can be target of antiviral drugs able to interact and block such a channel activity. Viroporins can be expressed in distinct phases of the viral infection and used with various modalities; hence, they can display different properties.

For example Influenza A virus encodes the M2 peptide, able to form an acid-activated proton channel that plays a key role in the viral genome uncoating: after internalization of the virus by endocytosis the pH of the endosomal vesicle is lowered. Activated by the acid pH, M2 shuttles protons from the endosome to the internal viral compartment, thus allowing the separation of the mRNA molecules from the M1 matrix envelope, and the viral genome introduction in the host cell nucleus. Another similar proton channel is the Hepatitis C virus encoded p7 peptide. Differently from Influenza A M2, p7 has been proposed to generate a proton leak that, at the late phase of the viral lifecycle, prevents acidification during exocytosis of new virions (A. L. Wozniak, et al., 2010).

Also the Human Immunodeficiency virus-1 (HIV-1) was found to encode for the viroporin Vpu, a single transmembrane domain peptide forming a non-selective channel. Vpu enhances the efficiency of viral particles release by a depolarization-stimulated exocytosis activity that contrast the host cell potassium currents, mainly from TASK K_{2p} channels, destabilizing in that way the electric field across a budding

membrane (K. Hsu, et al., 2010). Vpu is an “accessory protein”, not fundamental for the viral replication; however, it is interesting to notice that the HIV-2 strain, lacking the ion channel forming peptide, displays a lower pathogenicity.

During my PhD, I worked in the laboratory of Professor Anna Moroni (University of Milan, Italy) and that of Professor Gerhard Thiel (TU Darmstadt, Germany), in order to study and analyze the properties of two ion channels encoded by two different viruses: the miniature potassium channel PBCV-1 Kcv, encoded by the *Paramecium bursaria* Chlorella virus, and the Influenza A encoded PB1-F2 peptide.

7) PBCV-1 Kcv

Like other viral proteins, also viroporins can be smaller than functionally similar proteins encoded by cells, and their study can be helpful in the understanding of inherent properties of the central core that a family of proteins can share.

The viral channel PBCV-1 Kcv, thanks to its minimalistic structure, generated by the tetramerization of four identical subunits of 94 amino acids each, represents the module of the pore region of potassium channels. Hence, the interest in the study of its structural and functional properties can be useful not only for the elucidation of potassium channels behavior, but also for the reconstruction of the evolution of ion channels from a putative primitive protein.

PBCV-1

Paramecium bursaria Chlorella virus-1 (PBCV-1), encoding Kcv, is the prototypic member of a group of large (1900 Å in diameter at the five-fold axis) icosahedral, plaque-forming, dsDNA viruses, belonging to the family of Phycodnaviridae, that infect and replicate in the NC64A strain of the unicellular eukaryotic green algae Chlorella (Van Etten J.L., et al., 1991; Van Etten J.L., and Meints R. H., 1999) (Fig. 7). During the early phases of the viral infection, the potassium channel Kcv, inserted in the viral internal lipid membrane by fusion of the viral with the cell membrane, seems to depolarize the strongly negative membrane potential of the host cell (around -135mV, more negative than EK, the reversal potential of K^+). Such a depolarization lead to the opening of host potassium and chloride channels, and the consequent decrease of the turgor pressure by the loss of potassium and chloride ions from the cell. This event deny the removal of the virus from the host cell, and allows the injection of the negatively charged viral DNA molecules into the Cytosol (Mehmel M., et al., 2003).

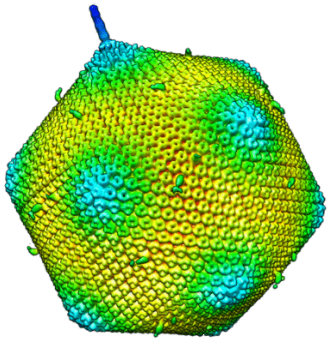

Fig 7: External envelope structure of *Paramecium bursaria* Chlorella virus-1.

Kcv macro currents

Kcv was shown to form functional potassium selective channels when expressed in heterologous expression systems, and its macro currents behavior was widely described with TE-Voltage Clamp experiments in *Xenopus laevis* oocytes (Fig. 8) (Pugge B., et al., 2000; Gazzarrini et al., 2002; Gazzarrini et al., 2006), and with whole-cell measurements when expressed in HEK 293 cells (Moroni et al., 2002). An instantaneous and a time-dependent kinetics are detectable from Kcv macro currents recorded from *Xenopus* Oocytes, resulting in a slow current decrease at positive voltages, and a current increase at negative potentials. Such a behavior is a function of the steady-state open Probability, that was found to increase at negative potentials, as described by the characteristic Kcv tails currents (Gazzarrini et al., 2002). It is interesting to notice that Kcv macro currents have an "inverted" kinetics behavior when expressed in HEK 293 cells: they display increase and decrease at respectively positive and negative membrane voltages (Hertel B., et al., 2006).

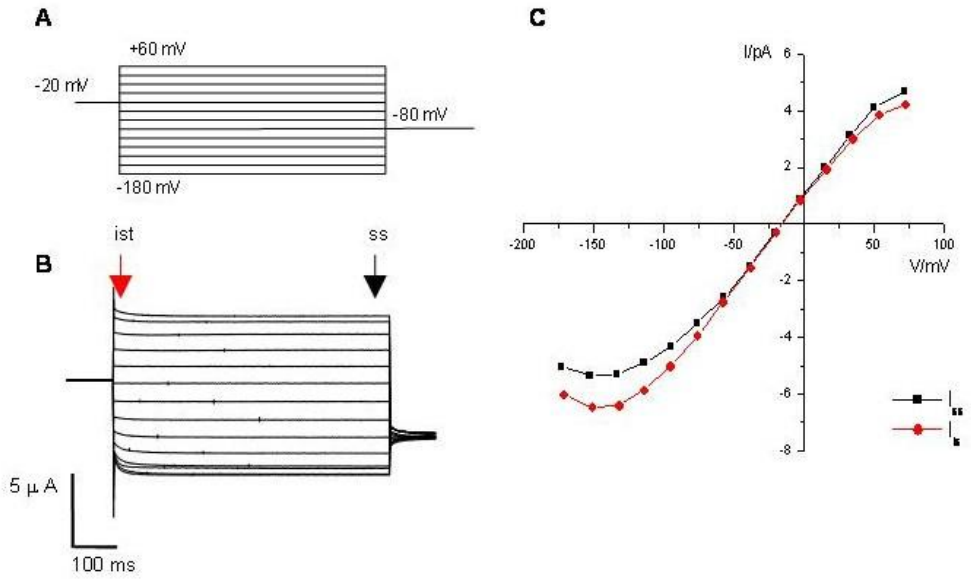

Fig. 8: PBCV-1 Kcv macro currents from *Xenopus laevis* oocytes (Gazzarrini et al., 2002).

A: Voltage protocol with -20mV holding potential, voltage steps of -20mV from +60 to -180mV, and tail potential of -80mV. B: Kcv macro currents resulting from the voltage protocol in A

C: Instantaneous (black) and time-dependent (red) IV curves obtained from Kcv macro currents in B.

Kcv currents are inactivated by Ba^{2+} in a voltage dependent manner (Plugge et al., 2000), while Ca^{2+} blocks the channel with a voltage-independent mechanism (Gazzarrini et al., 2002). The function of Kcv was found to be affected by Amantadine and Chloroquine. The first is a small molecule used as antiviral drug because of its ability to block some viral channels (Plugge B., et al., 2000; Syeda R., et al., 2008; Pinto L.H., et al., 2007), while Chloroquine is an anti-malarial drug able to block potassium selective channels such as that responsible of transient outward K^+ currents in cardiomyocytes (Wagner M., et al., 2010).

Single-channel measurements were so far obtained only in artificial membranes (bilayer), after expression and purification from *Pichia pastoris* (Pagliuca et al., 2007; Shim et al., 2007).

Kcv structure

By homology with the already known crystal structures of KirBac1.1 (Kuo et al., 2003), the monomer of Kcv is assumed to be formed by two transmembrane domains (TM1 and TM2), the filter region bearing the potassium channel signature sequence (TxxTxGY/FGD), an extracellular turret, and a 12-amino acids N-terminal domain that forms a cytosolic slide helix (Tayefeh et al., 2007) (Fig. 9). Despite Kcv minimalistic structure, the analysis of its macro currents suggests that gating mechanisms are at the bases of the slight voltage dependence of the Open Probability and the described activation and inactivation kinetics. It is therefore important to firstly establish which domains of the channel can be involved in conformational changes of the protein.

The short slide helix domain was found to be important for the channel functionality. When Kcv is deleted in the first 14 amino acids at the N-terminus, it is expressed and inserted in the plasma membrane with the same efficiency as the wt channel. However, the truncated protein does not induce a measurable current in transfected HEK 293 cells or *Xenopus* oocytes (Moroni A., et al., 2002). Hence, it was hypothesized that the slide helix plays a key role in the control of the structure of Kcv. This region contains two charged amino acids (a Lysine at position 6, and an Arginine at position 10). Unexpectedly, the substitution of these amino acids with non-charged amino acids doesn't affect the electrophysiological properties of Kcv. We have now evidences that movements of the slide helix in Kir channels are able to generate a rearrangement of the channel structure that is reflected on the selective Filter (Clarke O.B., et al., 2010). Such a conformational change results in the modulation of a gating mechanism. We can speculate that a similar property is at the basis of the behavior observed for Kcv.

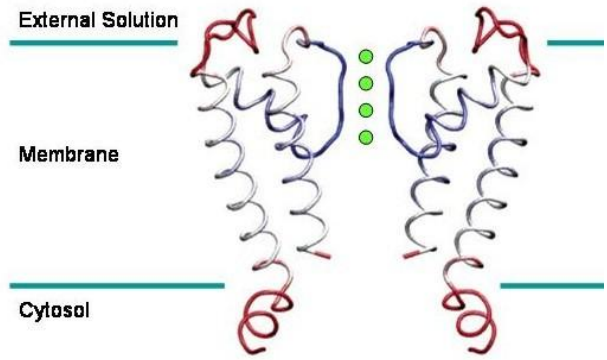

Fig. 9: Two opposite subunits of PBCV-1 Kcv inserted in the membrane (blue lines).
Four potassium ions are represented in the Filter (green dots).

Kcv TM2 gating

Also TM1 was found to be important in the regulation of the channel activity. This domain is connected with the slide helix by a Proline, that is responsible of the rotation of the cytosolic α helix respectively to the first transmembrane domain. The substitution of the kink-forming Proline with an Alanine generates the elongation of TM1. The resulting conformational change is responsible for different electrophysiological properties of the mutant channel in comparison with that of Kcv wt. HEK 293 cells transfected with Kcv P13A display at negative potentials a higher conductance level and activation kinetics instead of inactivation kinetics (Hertel B., et al., 2006). A modification of a gating mechanism must be considered on the basis of this knowledge.

Molecular Dynamic simulation (MDS) gave an important contribution to the interpretation of the P13A mutant channel behavior. A comparison of MDS on Kcv wt and Kcv P13A revealed that a higher distance between the N- and the C-terminus interferes with the formation of salt bridges between these two domains, resulting in a higher flexibility of the C-terminus second transmembrane domain (Tayefeh S., et al., 2007). This domain (TM2) is a 19 amino acid long α-helix, and seems, at a first glance, to be too short to cross the C-terminal portions forming the same bundle crossing structure found in the KcsA crystal (McKinnon, 1998). However, MDS data on Kcv wt revealed that these TM2 helices, provided by the channel tetramerization, can come close enough to reduce the pore diameter at the cytosolic entrance and slow down the ion flux (Tayefeh S., et al., 2007). On the contrary, the simulation of the mutant channel behavior revealed that the elongation of TM1 results in an increased pore diameter. A possible explanation of the electrophysiological data came from the idea that the position of the TM2 domain is important in the modulation of a gating mechanism similar to the well known bundle crossing gating in KcsA.

Additional evidences of a “minimal bundle crossing” mechanism at the TM2 level required the measure of single channel activity from the wt and the mutant channels, and the comparison of parameters such as the single channel conductance (g) and open probability (P. open).

Kcv filter gating

The growing evidences that important gating mechanisms are localized at the level of the filter region of potassium channels (Cuello L.G., et al 2010; Rotem D., et al., 2010), focused our attention on the possible role of this domain also on Kcv gating. As discussed in the Introduction, the mutation of a single amino acid in the selectivity filter of KcsA (E71A) was shown regulate the C-type inactivation, leading to a strong increase of the single-channel open probability (Cordero-Morales et al., 2007). In KcsA wt the interaction of the Filter helix and the Filter is provided by a salt bridge between the Glutamic acid at position 71 and the Aspartate at position 80 (Fig. 10). The modulation of the C-type inactivation is due to the loss of this interaction in the mutant channel. However, single-channel traces recorded from the corresponding mutant of Kcv (T59A) didn't display an appreciable increase of the open probability or a change in the single-channel conductance (data not shown). We concluded that the structure of the filter region doesn't control the slow gating mechanism as in KcsA, without excluding the possibility that the same region could affect other gating mechanisms.

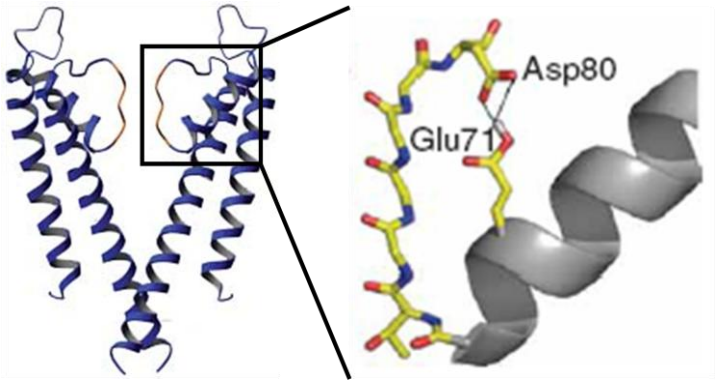

Fig. 10: KcsA Crystal structures of the filter and helix filter regions. Glutamic acid at position 71, and Aspartate at position 80 are highlighted (Cordero-Morales et al., 2007).

KcsA crystal data demonstrated that the potassium concentration could affect the structure of the filter, and that in low potassium this region passes from a conductive to a collapsed non conductive conformation (McKinnon et al., 2001). According to these data, the behavior of another potassium channel, MaxiK, measured with different KCl concentrations, was explained by the Ion Depletion Model: fast closure events at extreme membrane potentials can be found when measuring in low potassium conditions, but not in high potassium (Schroeder I. and Hansen U.P., 2007).

Measuring Kcv single-channel traces, we found that the IV Curve has an ohmic behavior at voltages around the reversal potential, while a decrease of conductance occurs at extreme potentials. The analysis of single-

channel opening events revealed that at extreme potentials an increase in noise characterize the current level of the open-channel, and a mechanism of fast flickering was hypothesized to occur at extreme voltages, as a consequence of the ion depletion of the Filter region. β-distribution analysis of Kcv single-channel traces, done in collaboration with Schroeder I. and Hansen P.U., confirmed that an ion depletion mechanism can be at the basis of the negative slope conductance displayed by of the single-channel IV Curve at extreme potentials.

In order to confirm the β-distribution analysis, we measured Kcv single channel traces in different ionic conditions, increasing the potassium concentration of the internal and external solutions.

The work presented here is directed to the characterization of gating modalities in Kcv, by studying the regions putatively involved in conformational changes of the channel, the study of mutants of Kcv displaying different properties, and by the analysis of the different environmental conditions that can affect the channel behavior. For this study, I took advantage of the TE-Voltage Clamp technique, and the Patch Clamp technique, in order to evaluate the properties of the measured channels in function of the electrophysiological parameters characterizing macro currents and single channel traces.

8) Influenza A virus PB1-F2

Influenza A virus

Influenza A viruses are important pathogens replicating in both humans and animals. Their infections caused the strongest and most deadly pandemic in 1918-1919, killing around 50 million people worldwide. Many of those deaths were associated with secondary bacterial pneumonia (Beveridge W.I., 1991; Johnson N.P. and Muller J., 2002), and an increased lung pathology. Bacterial infection, connected with Influenza A, were found in mice models and humans lungs, from *Streptococcus pneumoniae*, *Staphylococcus aureus* and *Haemophilus influenza* (Sethi S., et al., 2002; Zamarin D., et al., 2006; McAuley J.L., et al., 2007).

Influenza A are RNA viruses with a genome composed by 8 RNA molecules with negative polarity. These molecules were thought to encode for 10 proteins (named PB1, PB2, PA, HA, NP, NA, M1, M2, NS1, NS2) (Fig. 11); however, in the latest years, new proteins were found through a search of CD8+ T-cell reactive epitopes. One of these proteins is PB1-F2, deriving from the shift of one nucleotide (reading frame shift) of the gene encoding PB1 a protein that complex with PB2 and PA forming an RNA transcriptase together with NP-mRNA complexes.

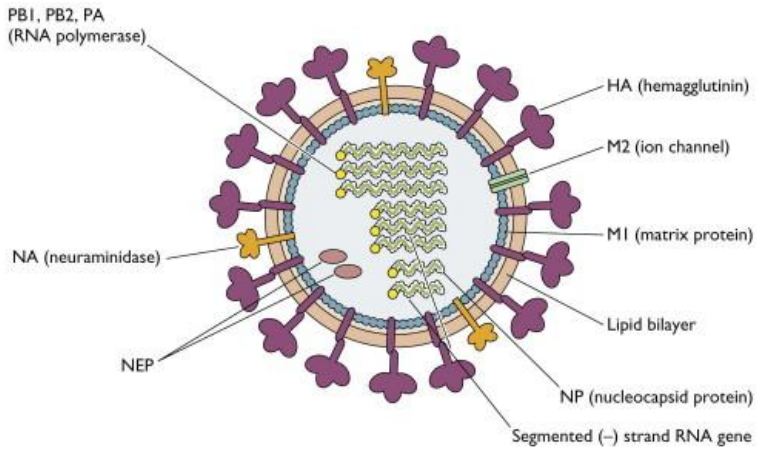

Fig. 11: Influenza A virus. Viral proteins and genome are indicated.

PB1-F2 as pathogenic factor

PB1-F2 expression was found to be associated with a significant morbidity and mortality increase in comparison with non expressing viral strains. This protein can indeed induce DNA damage and tumor necrosis, and trigger apoptotic signals in a cell-dependent manner (Zamarin D., et al., 2005). The viral peptide is composed by three domains: a C-terminus α-helix that confers the propensity to insert in lipid membranes, and where a minimal Mitochondrial Targeting Sequence (MTS) was found (Gibbs J.S., et al., 2003), and two N-terminus domains, potentially involved in the interaction with mitochondrial membrane proteins such as ANT3 or VDAC1 (Zamarin D., et al., 2005). The structure of the peptide is able to switch from a disordered and coiled state in an hydrophilic environment, to β-sheet or α-helix when inserted in a lipid membrane (Chevalier C. et al., 2010).

PB1-F2 was shown to increase the permeability of lipid membranes, generating random fluctuations between multiple undefined conductance levels. A channel like behavior was not described; instead, the formation of lipidic pores was suggested (Chanturiya A.N., et al., 2004). PB1-F2 is thought to initiate an apoptotic pathway through the depolarization of the mitochondrial membrane: it is not clear whether an interaction with ANT3 and VDAC1, or the formation of pore, is at the base of the PB1-F2 induced Cytocrome C release from isolated mitochondria (Zamarin D., et al, 2005). The viral peptide was found not only in the internal and external mitochondrial membrane, but also in the nucleus and cytosol of infected cells, where a possible role during the viral infection cycle has not been described so far. The induced cell death mechanism is probably activated in a late phase of the viral infection, and can be related to a decreased ability of the immune response by the infected organism.

Not all Influenza A viral strains encode the full length PB1-F2 peptide: the 76,8% of the European swine viruses isolated from 1979 to 2009 present a full length protein, that is 87 amino acids long in some viral strains, and 90 amino acids long in others. The remaining 23,2% viral strains encode a truncated version of the viral peptide, from 8 to 81 amino acids (Zell R., et al., 2006, 2007). For example the swine H1N1 viruses presents three stop codons in the gene encoding PB1-F2 peptide, and a truncated not-functional version of only 11 amino acids is synthesized.

H1N1 swine flu PB1-F2

On the basis of this knowledge, and considering the ability of viruses to easily mutate their genome, we were wondering whether a new functional peptide could arise from mutations that, by removing the first two stop codons in the H1N1 swine flu PB1-F2 encoding sequence, allow the synthesis of the first 87 amino acids. On this purpose, a new sequence (aPB1-F2sf) was created converting the two stop codons into the most likely amino acids that a random mutation can introduce; in that way we generated the PB1-F2 peptide that a new swine Flu viral strain would possibly synthesize in the future.

In the laboratory of Professor Gerhard Thiel (TU Darmstadt, Germany), the ability of PB1-F2 peptides to generate non-selective ion channel activity in artificial lipid bilayer was previously demonstrated: viral peptides from three different Influenza A strains (PB1-$F2_{PR8}$ from an Influenza A Puerto Rico strain (H1N1), PB1-$F2_{SF2}$ from a Spanish flu isolate (H1N1), and PB1-$F2_{BF2}$ from 13 different bird flu strains(H1N5)) was shown to display step like current fluctuations between a close and different defined open states (Henkel M., et al. 2010). In order to verify whether the mutated swine flu peptide (aPB1-F2sf) share similar characteristics with other PB1-F2 proteins, I tested its propensity to generate channel like activity in artificial lipid bilayer, comparing its electrophysiological properties with that of the other already characterized peptides.

The finding that also aPB1-F2sf can generate a functional ion channel was associated with the possibility that a new swine flu virus could display a higher pathogenicity in the future. We wanted define then whether the biological role of these peptides during the viral infection cycle would be confined to the destabilization of the mitochondrial membrane, or if its channel activity could be important also in other cell membranes, or during other viral infection phases.

For this purpose, I measured whole-cell currents from different mammalian cell strains, before and after adding aPB1-F2sf at different concentrations in the external medium.

The final goal was to determine whether a physiological signal, beside the membrane potential changes, could be trigged by the insertion of the viral peptide in the cell membrane. We hypothesized that an increase of Ca^{2+} permeability could result from its insertion into the cell membrane; it is known in fact that variations of the cytosolic Ca^{2+} concentration can initiate a multitude of events with strong effects on the cell physiology.

I present here experiments where variations of the cytosolic Ca^{2+} concentration was measured, upon addition of aPB1-F2sf to the external medium of the same cells line previously used for electrophysiological measurements.

PBCV-1 Kcv

Materials and Methods

PBCV-1 Kcv

1) *Xenopus laevis* Oocytes preparation for electrophysiological measurements

Xenopus laevis Oocytes are used since '70s as system for the expression of heterologous proteins. They are extracted from adult females following the standard methods discussed in Plugge et al., 2000: *Xenopus* are anesthetized with 0,7 g/l of Tricaine methanesulfonate and, once the loss of reaction to stimuli is verified, an incision is made at the level of the abdominal muscles. After oocytes extraction, stitches are made in order to reconstitute the cut muscles and skin. Extracted oocytes are treated with collagenase (type 1A, Sigma) 300 u/ml for 10 min at 16°C, and then washed with 500 ml of the physiological solution OR2 (82,5 mM NaCl, 2 mM KCl, 1 mM $MgCl_2$, and 5 mM HEPES, adjusted to pH 7.5 with NaOH). This solution doesn't contain calcium, known to increase collagenase activity. Oocytes are surrounded by a vitelline membrane, around the plasma membrane, and an external follinic membrane; the follinic membrane, partially digested by collagenase, is mechanically removed by the passage of oocytes through narrowed Pasteur pipettes. Oocytes are now ready for cRNA injection.

PBCV-1 *kcv* cDNA is cloned into pSGEM vector (a modified version of pGEM-HE; provided by M. Hollmann, Max Planck Institute for Experimental Medicine, Gottingen, Germany), and capped cRNA is transcribed in vitro using T7 RNA polymerase (Promega) and injected (50 ng/oocyte) into extracted oocytes. Injected oocytes are then incubated at 19°C in ND96, another physiological solution containing also calcium, (96 mM NaCl, 2 mM KCl, 1.8 mM CaCl2, 1 mM MgCl2, and 5 mM HEPES, adjusted to pH 7.5 with NaOH). The experiments were performed 2–7 d after injection.

Patch Clamp measurements, on the contrary of TE- Voltage Clamp experiments, require the manual removal of the vitelline membrane.

2) Electrophysiology

Oocytes expression level is monitored by recording currents in two-electrode voltage clamp configuration (Geneclamp 500; MDS Analytical Technologies). Electrodes are filled with 3 M KCl and have a resistance of 0.4–0.8 MΩ in 50 mM KCl. The oocytes are perfused at room temperature with a standard bath solution containing 50 mM KCl, 1.8 mM $CaCl_2$, 1 mM $MgCl_2$, and 5 mM HEPES (pH adjusted to 7.4 with KOH and osmolarity to 215 mOsm with mannitol). Oocytes showing >6 µA of current at V = 60 mV are used for patch clamp experiments. Patch pipettes are pulled from thin-walled borosilicate glass capillaries, coated with Sylgard (Corning), and fire-polished to a final resistance of 0.8–1 MΩ for macro-currents and 8–15 MΩ for single-channel experiments. Standard pipette solution contains 100 mM KCl, 1.8 mM $CaCl_2$, 1 mM $MgCl_2$, and 10 mM HEPES (pH to 7.4 with KOH). Macro-currents and single-channel recordings were made in cell-attached and inside-out configurations. The standard bath solution contains 100 mM KCl, 1 mM $MgCl_2$, 1 mM EGTA, and 10 mM HEPES (pH to 7.4 with KOH). Experiments are performed at room temperature after removal of the vitelline membrane from oocytes in a hyperosmotic solution (ND96 solution plus 100 mM NaCl). Currents were recorded with a Dagan 3900 amplifier, and data were low-pass filtered at 1 kHz and digitized at a sampling rate of 10 kHz for macro-currents. For single-channel recordings, the four-pole Bessel filter was set to 2–5 kHz and the sampling rate to 10–25 kHz. Different solutions are fed by gravity, and solution change takes no more than 20 s. Single-channel analysis is done using pCLAMP 9.2 (MDS Analytical Technologies) with the threshold-based algorithm, except for fast-gating analysis (see below).

3) Evaluation of fast gating

The measured current in the open state of the channel displays increased noise if gating is faster than can be resolved by the recording apparatus. Often, the value of the apparent single-channel current, I_{app}, extracted from such records is smaller than the value of the true single-channel current, I_{true} (which would be measured if the temporal resolution of the recording apparatus were high enough). Both I_{true} and I_{app} require clear adequate algorithms as a basis for their determinations from measured time series (Hansen et al., 2003; Schroeder and Hansen, 2006, 2007, 2008). Base line drift, membrane flickering, endogenous channels, and other artifacts would distort the analysis. Thus, all data had to be closely inspected and cleaned manually from sections showing these kinds of artifacts (Sigworth, 1985). Sections of fast gating were extracted from the measured time series (excluding sections of obviously closed states) by means of a Hinkley detector in the program Kiel-Patch (Schultze and Draber, 1993). These "cleaned time series" are used to generate the open-point histogram (distribution per-level; Schröder et al., 2004) of the apparent open state.

4) Determination of the apparent single-channel current, *Iapp*

The apparent current I_{app} as obtained from the maximum of the amplitude histograms strongly depends on the corner frequency of the filter of the recording setup (Fig. 2 in Schroeder and Hansen, 2008). Nevertheless, it can reach a well-defined asymptotic value when the corner frequency of the electronic filter is low enough. This value is used here because it corresponds to the instantaneous current level obtained from whole cell recordings. Because the cleaned time series comprise only sections of fast gating, they constitute a stationary time series of great length, thus enabling the application of filtering (moving average in Kiel-Patch) of sufficient low frequency (mainly 500 Hz) and the determination of the asymptotic value of I_{app}.

The experiments in MaxiK were done in HEK293 cells with a filter corner frequency of 50 kHz, whereas a 5-kHz filter was used here for Kcv. To test whether the different experimental conditions may have an influence, the data of MaxiK (Schroeder and Hansen, 2007) were refiltered by a digital 5-kHz four-pole Bessel filter. The refiltered data led to the same results as the 50-kHz data (not depicted). This indicates that differences in the behavior of Kcv and MaxiK are not caused by the different temporal resolution of measurements in Kcv and MaxiK.

5) Determination of the true single-channel current, *Itrue*, and of the rate constants of an O-C model of fast gating

The open-state amplitude histogram of I_{app} as obtained from the bursts is broader than that of the base line, and its curve shape may deviate from that of a Gaussian distribution (Fitzhugh, 1983; Yellen, 1984; Klieber and Gradmann, 1993) (see Fig. 4 A). These so-called β distributions can be used to determine the true single channel current and the rate constants of the underlying Markov model (Schroeder and Hansen, 2006, 2007, 2008). Schroeder and Hansen (2006) have shown that it is sufficient to use a truncated Markov model (two states: O-C) for the analysis of the bursts in the time series. A simplex algorithm (Caceci and Cacheris, 1984) is used to fit the "theoretical" open-point histogram obtained from the two-state model to the open-point histogram of the measured data. Unfortunately, there is no straightforward procedure to calculate β distributions obtained from higher-order filters (Riessner, 1998). Thus, simulations instead of deterministic algorithms are used to provide the theoretical curves. This is quite time-consuming during a fitting routine, but it turned out to be the most efficient way to resolve fast flickering. The fit algorithm has to determine three parameters of the O-C model: the true open-channel current I_{true} and the rate constants K_{OC} and K_{CO}. Even though it provides the automatic determination of all three parameters (Schroeder and Hansen, 2006), the fitting procedure treats I_{true} and K_{CO} and K_{OC} differently. The current is used as a fixed parameter that is changed stepwise in subsequent fits. The computer determined the best set of K_{OC} and K_{CO} for each suggested current. The resulting plot "error sum versus assumed I_{true}" is very helpful for the estimation of the reliability of the fit (see Fig. 4 B). In the case of good data, a pronounced minimum is found, and the location of this minimum is taken as the true single-channel current (see Fig. 4 B). The rate constants K_{CO} and K_{OC} of the related fit were used for Fig. 5 B. The software for Kiel-Patch and for the β fits (downhill) is available at www.zbm.uni-kiel.de/aghansen/software.html.

Results

PBCV-1 Kcv

Compared with K^+ channels from pro- and eukaryotes, the viral channel Kcv is small indeed (Plugge et al., 2000). But in spite of its minimalistic structure, Kcv is characterized by voltage dependent gating mechanisms, detectable by the analysis of its currents. The results presented here are addressed to the description of the biophysical aspects underlying these characteristics of Kcv. Starting from the description of its macro currents, and the knowledge that could be deduced from their analysis, we found which domains of the channel are involved in structural changes characteristic of gating mechanisms. On this basis we could then demonstrate the validity of our model by modulating and interacting with the described mechanisms. This findings can become important in the future by the understanding and possible applications on Kcv and other potassium channels.

Two electrode Voltage Clamp macro currents recorded in Kcv expressing *Xenopus* oocytes (fig. 12a) are characterized by an instantaneous and a time dependent conductance, which display current decrease at positive voltages, and current increase at negative voltages. The Current/Voltage relationship of the instantaneous component (fig. 12b) is linear in a range of ±40 mV around the reversal potential, and reveals a conductance decrease at extreme potentials.

Kcv macro currents recorded by the Patch Clamp technique in Inside-Out configuration (fig. 12c) reveal that Kcv maintains the same behavior after excision of the Patch from the oocyte surface, as shown by the relative IV Curve (fig. 12d), showing that the internal cytosolic environment is not responsible for Kcv gating properties. However, the two IV curves from TE-Voltage Clamp and Patch-Clamp measurements are not identical: macro-patch currents display current decrease at extreme potential, but not the same negative slope conductance that characterizes TE-Voltage Clamp currents. This difference can be related to the lower current to noise ratio of macro-patches in comparison with Voltage Clamp recordings, probably related to an instability of the patch and the passage of leakage currents.

In order to establish whether these are inherent channel properties, I used the Patch Clamp technique to measure Kcv single channel behavior.

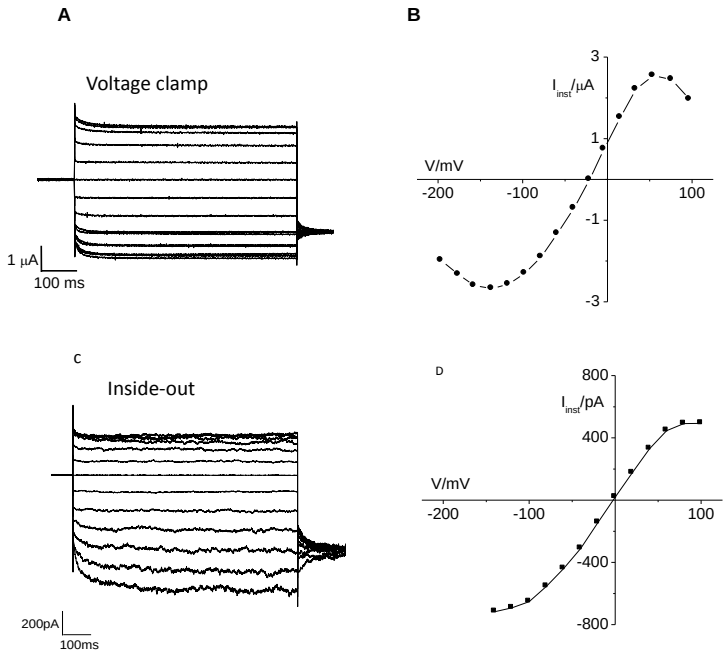

Fig. 12:

A) TE Voltage Clamp Kcv macro currents recorded from Xenopus oocyte, showing inactivation at positive potentials, activation at negative potentials, and conductance decrease at both positive and negative potentials.

B) Current/Voltage relationship from TE Voltage Clamp measurements.

C) Kcv macro currents recorded from Xenopus oocyte with Patch Clamp technique in Inside-Out configuration. The excision of the Patch from the cell doesn't affect macro currents features.

D) IV Curve from Patch Clamp recorded macro currents.

In fig. 13a single channel fluctuations between close and open state are detectable. Plotting the open-state current level against membrane potential (fig. 13b), we found a current decrease at extreme potentials as described for macro currents (fig. 12b). This finding demonstrates that the characteristic shape of the IV Curve is due to single-channel behavior. The calculated single-channel conductance of Kcv was 114 ± 11 pS.

The same I-V relation (fig. 14) was obtained in inside-out configuration in different ionic conditions, in order to discriminate the effect of the internal solution components, and remove all possible sources of channel block. In the most of the measurements the bath solution contained KCl 100mM, $MgCl_2$ 1mM, EGTA 1mM and HEPES 10mM; just a possible calcium block is thereby excluded. In other experiments the bath solution was substituted with one containing KCl 100mM, no $MgCl_2$, EDTA 1mM instead of EGTA, and

HEPES 10mM (data not shown), and another solution with just KCl 100mM, and HEPES 1mM instead of 10mM (fig. 14, red). With the two last solutions a blocking effect from magnesium, EGTA, or HEPES can be discarded, concluding that the negative slope conductance of the outward single-channel currents is an inherent property of Kcv, not related to an ion block mechanism.

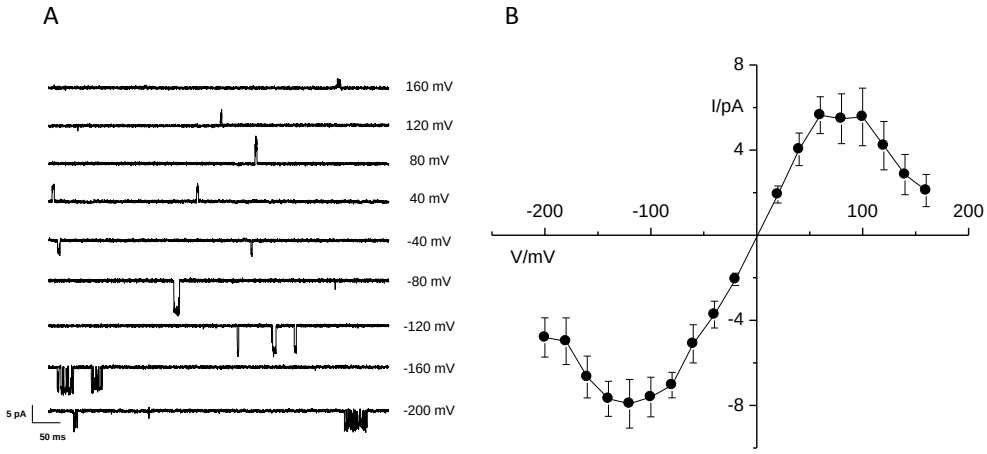

Fig. 13:

A) Kcv Single channel traces at different membrane potentials.

B) Kcv Single channel IV Curve (g=114 ± 11 pS).

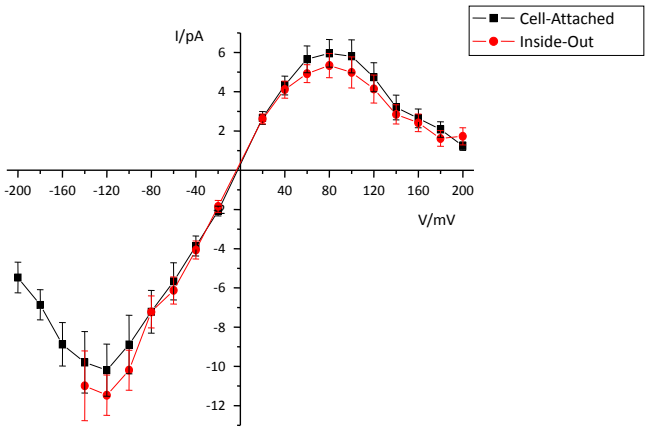

Fig 14: PBCV-1 Kcv single channel IV curves in Cell-Attached (black) and Inside-Out configurations (red). In the Inside-Out experiment the bath solution is: KCl 100mM, HEPES 1mM, MgCl2 0mM, EDTA 0mM.

A more detailed analysis of Kcv single channel traces reveals that at least two mechanisms of gating are involved (fig. 15): a Fast gating mechanism, responsible of the so-called “Fast Flickering behavior”, and a Slow gating mechanism, which give rise to closures in the range of msec.

During my PhD, I’ve been working on the analysis of both these two aspects of Kcv behavior.

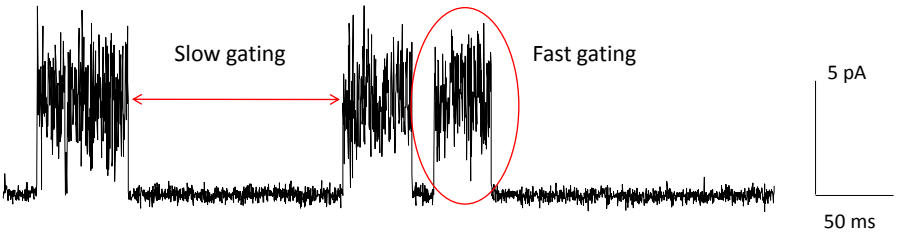

Fig 15: Kcv Single channel trace recorded at +100 mV, showing Fast and Slow gating mechanisms.

Fast Gating.

The temporal resolution of Patch-Clamp set-ups is limited by two features: a) the response time or corner frequency (cut-off frequency) of the electronic circuit and b) the signal to noise ratio. This two problems are coupled, and increasing the corner frequency also increases the noise of the amplifier. Thus the frequency response of the amplifier is limited by an electronic filter with selectable corner frequency, in order to keep the noise at a tolerable level.

The Fast gating mechanism is responsible of opening-closure events which occur with a frequency higher than the corner frequency of the electronic filter of the recording setup; thus, these events are too fast to be fully resolved. Instead fast gating is indicated by two effects: the measured single channel opening events appear more noisy than the baseline, and the open channel current level seems to decrease at extreme potentials, as compared to recordings without fast gating (fig. 16). As shown in fig. 16, the fast gating mechanism is not symmetrical: it is more pronounced at extreme positive than at negative voltages.

The reconstruction of the full opening events could be possible by the usage of β-distribution analysis (fig. 17): the frequency of occurrence of data points in a window of nominal currents is plotted versus the mean value of the current in that interval (Point amplitude distribution, fig. 17a), producing the β-distribution. In records without fast gating the amplitude histogram is a sum of Gaussian distributions. In the presence of fast gating the width of the Gaussian distribution can be widened as compared to that of the baseline or can become skewed. Those amplitude histogram deviating from the normal Gaussian distributions are called β-distribution (FitzHugh R., 1983). In some cases it is still possible to distinguish between the points belonging to the close-state level (fig. 17a, black line), and those belonging to the open-state level (fig. 17a, red). In others cases, open and closed states may be merged in one distribution making the analysis more complicated.

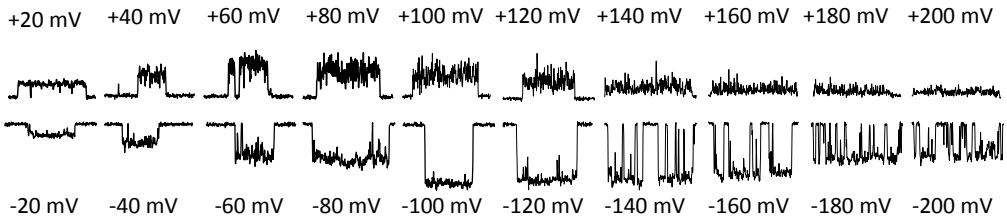

Fig 16: Kcv Single channel opening events showing a more pronounced Fast gating mechanism at extreme positive potentials.

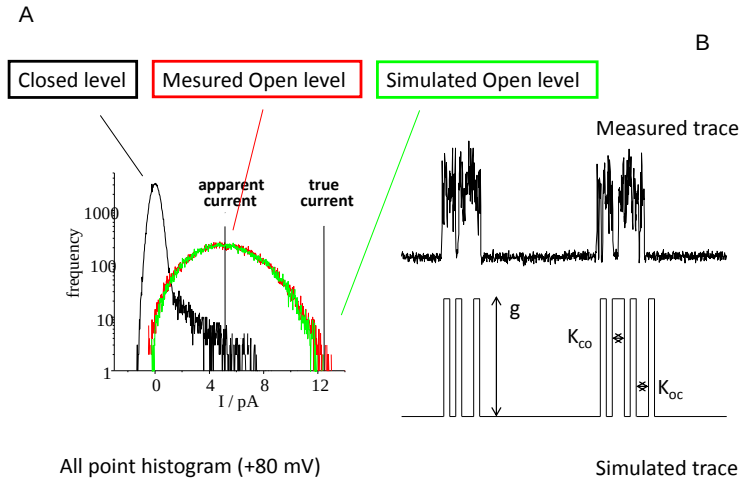

Fig 17: β-distribution analysis.

A) Point amplitude distributions from a time series recorded at +80 mV are shown (black line, close level; red line, open level).

B) Kcv Single channel opening events recorded at +80 mV, and a schematic representation of the same simulated trace.

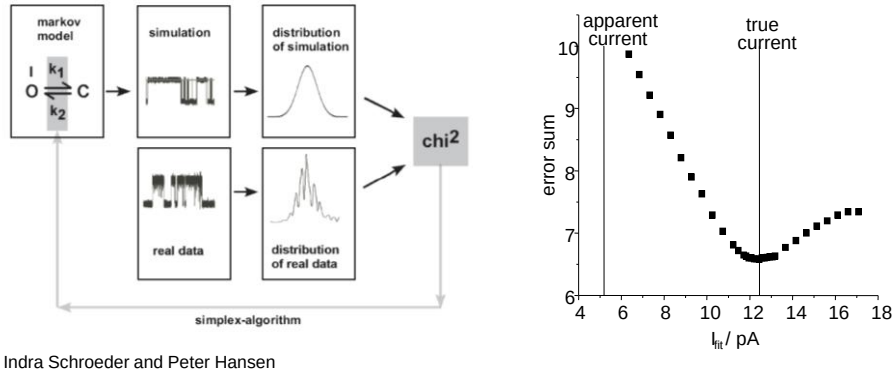

Fig 18: Minimum error sum. Dependence of the error sum of the fit on the assumed Current value. I_{true} = 12.5pA (vertical line) is the value of Current that gives the minimum value in the error sum in this example.

The canonical description of gating is based on so-called Markov models (Colquhoun D. and Hawkes A.G. 1990). For fast gating, a truncated two-state Markov model is sufficient. It is assumed that the channel oscillates between an open (O) and a closed state (C). The rate constants k_{OC} and k_{CO} describe the probabilities of transition between these states, and they have to be determined from the measured data. Since there is no analytical approach to calculate β-distributions, simulations have to be used as follows: starting from a truncated Markov model with just two states (Open and Close), a simulated time series is generated (fig. 17b), and subject to the same sampling and filter frequency as the measured data have

been. For this simulation, three parameters are adjusted until reaching the minimum value of error sum (fig. 18), when the β-distribution of the measured open level and that of the simulated open level are as similar as possible (fig. 17a). Those parameters are k_{OC} and k_{CO}, as mentioned above, and the "true single-channel current" (I_{true} which often is unknown because averaging in the electronic filter reduces the true single-channel current to I_{app}, the measured "apparent single-channel current").

As result of β-distribution analysis, it is possible to define the real current level (I_{true}), and the kinetics constants relative to the opening and closure events (k_{CO} and k_{OC} respectively). The real current level, as expected, results to be higher than the measured one (I_{app}, fig. 19a), and the relative IV Curve lacks the negative slope conductance at extreme positive potentials that characterize the IV curve from I_{app}. Even removing the contribution of the Fast gating mechanism on the IV plot, we can estimate a conductance decrease at extreme positive voltages, that must be explained as result of a mechanism different from that one causing the Fast gating one.

Plotting the voltage dependence of the rate constants (fig. 19b) demonstrates that their values reside in a range undetectable for the measuring setup (sampling frequency of 10KHz). The increase of the closure rate (k_{oc}) at extreme potentials is symmetrical at positive and negative voltages; on the contrary, the opening rate values (k_{co}) keep on decreasing at extreme positive voltages, inducing the channel to close more frequently and generating the apparent current decrease at extreme positive voltages.

The gating factor R is calculated as I_{true}/I_{app} (fig. 19c). Kcv gating factor increases at extreme positive voltages, highlighting the increasing difference between the true and the apparent current levels. The same gating factor is plotted for the human K^+ channel MaxiK (Schroeder and Hansen, 2007) at different KCl concentration of the experimental solution. At higher potassium concentrations the gating factor tends to decrease, as if K^+ was able to stabilize the channel in the open conformation.

To explain these data the “Ion depletion model” was hypothesized (fig. 20): at extreme positive potentials the rate of expulsion of potassium ions from the Filter region to the external solution is higher than the rate of refilling of ions from the Cavity to the Filter. As shown by crystal structure data (Zhou Y. And MacKinnon R., 2003), when the Filter is empty it can collapse and thus undergoing in a non-conductive state. This mechanism could be responsible of fast opening and closure events. Following this hypothesis, a higher K^+ concentration in the internal solution should balance the rate of refilling of ions from the Cavity to the Filter and the rate of expulsion of potassium ions from the Filter to the external solution. Single-channel measurements had been done in order to verify the validity of the Ion depletion model on Kcv.

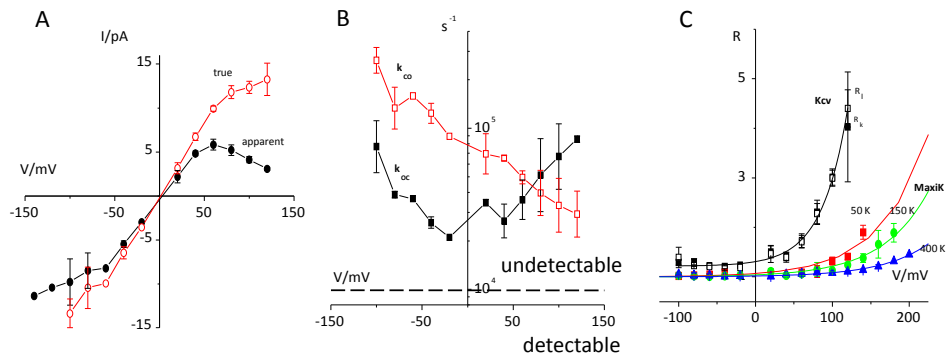

I/V curves of Iapp. and Itrue

Voltage dependance of Koc and Kco
Sampling = 10KHz = 1/100 µs

Gating factor (R)

Fig 19: IV curves of "apparent" and "true" currents (A), k_{oc} and k_{co} voltage dependence (B), and MaxiK and Kcv "gating factors" R (C), from β-distribution analysis.

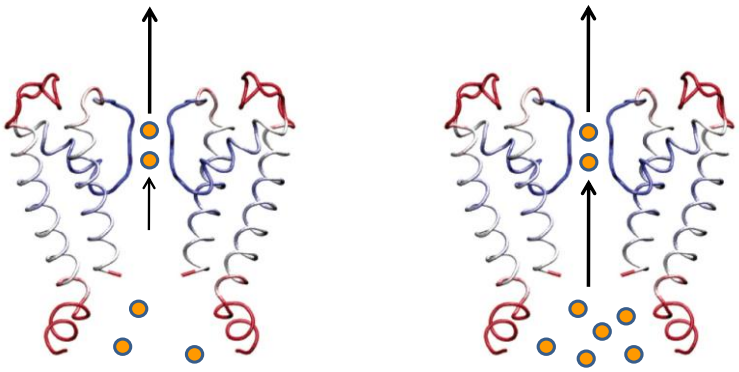

Low potassium

High potassium

Fig 20: Ion depletion model. Two opposite subunits of Kcv are represented, with potassium ions from the internal solution (orange dots), and arrows indicating the rates of refilling and expulsion of ions from the Filter region. Two conditions of low potassium (left) and high potassium (right) are represented.

Single-channel IV Curves from the same Patch are shown in Cell-Attached and in Inside-Out configurations (fig. 21a, black and red respectively). The cytosolic K^+ concentration in oocytes is around 100 mM, and the single channel conductance decrease at extreme positive potentials, as discussed above; in Inside-Out configuration the Patch was plunged in a bath solution containing KCl 300 mM. Confirming the Ion depletion model, at higher internal K^+ concentration, the IV Curve doesn't display negative slope conductance at extreme positive potentials, as shown also by plotting the conductance against the

membrane potential at positive voltages (fig. 21b). Fig. 21c show Kcv single channel traces at voltages at approximately the same distance from the calculated reversal potential (+80 mV for the Cell-Attached measurement; +60 mV for the Inside-Out measurement); opening events measured with higher internal K^+ concentration are less noisy, and their average current level is higher; however, events with unreduced noise still occur, demonstrating that KCl 300 mM is not enough concentrated to completely stabilize Kcv Filter region preventing fast closures. The same result is confirmed by measurements where the internal K^+ concentration was changed from 100 mM to 250 mM (fig. 22a, b).

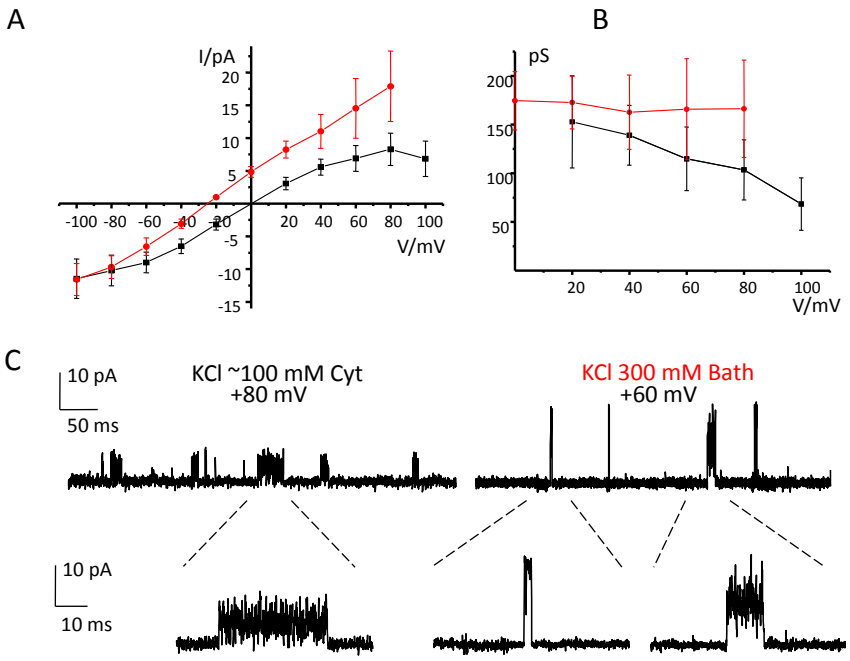

Fig 21: Kcv Single channel IV Curves (A) and Single channel Conductance (B) recorded with K^+ ~100mM (black) in the Cytosolic solution and K^+ 300mM (red) in the bath solution (Inside-Out configuration). At higher internal K^+ concentration, the IV Curve doesn't display conductance decrease at extreme positive potentials.

(C) Kcv Single channel traces and Single channel opening events (enlarged) recorded with the two different solutions.

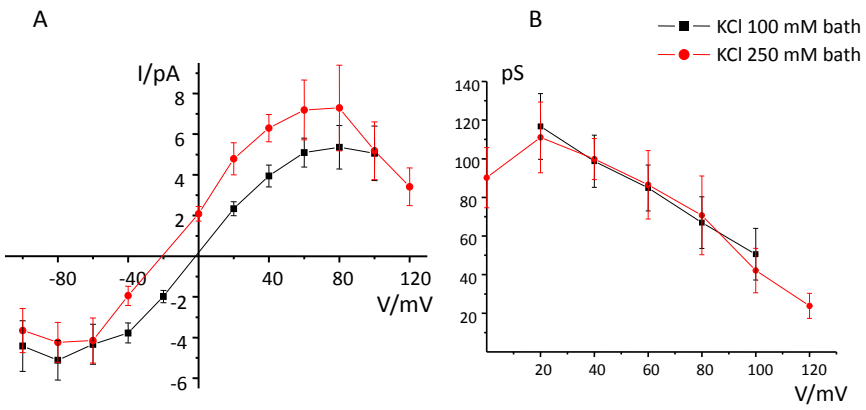

Fig 22: Kcv single-channel IV Curves (A) and single-channel Conductance (B) recorded with K^+ 100mM (black) or K^+ 250mM (red) in the bath solution. K^+ 250mM in the bath solution doesn't change the single-channel IV curve shape, and doesn't affect the single-channel conductance.

The apparent decrease in conductance at extreme potentials and the accompanying increase in noise are always observed and can be considered characteristic of Kcv, but the polarity of the voltage effect is not constant. The most common behavior is that presented in fig. 16. However, fig. 23 shows opening events where the Fast flickering behavior is more pronounced at negative than at positive potentials. Different behaviors are usually found in different batches of oocytes, and could be explained with a different membrane environment that could influence Kcv activity. Fig. 24 shows that it is possible to remove the negative slope conductance also at negative voltages: two Patches from the same oocyte are compared, recorded one with 100 mM KCl (fig. 24a, b, black) and the other with 300 mM KCl (fig. 24a, b, red) in the Pipette solution. The comparison of opening events at approximately the same driving force (-60 mV with 100 mM KCl, and -40 mV with 300 mM KCl) demonstrate that the increasing external K^+ concentration, differently from the internal K^+ concentration effect, strongly reduces the current noise level in an homogenous way.

All these data support the view that the stability of the Filter of K^+ channels is crucial for their behavior, and that a Fast gating mechanism could be affected interacting with this region.

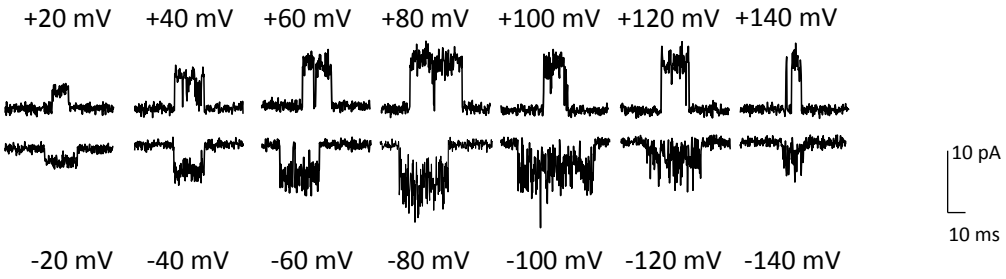

Fig 23: “Inward flickering”. Fast gating mechanism is more pronounced at extreme negative potentials.

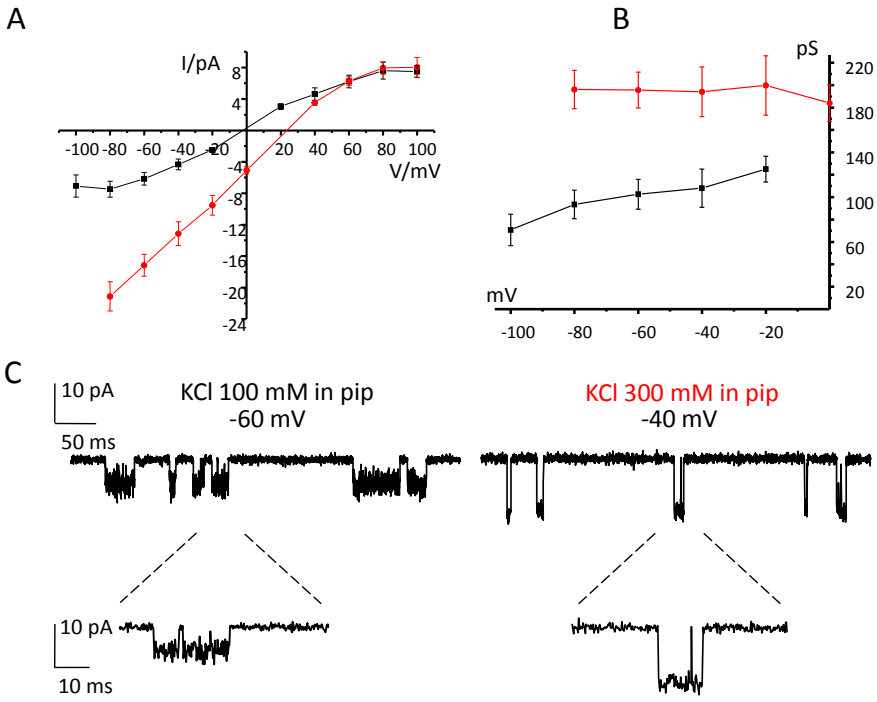

Fig 24: Kcv Single channel IV Curves (A) and single-channel Conductance (B) recorded with K^+ 100mM (black) and K^+ 300mM (red) in the pipette solution. At higher external K^+ concentration, the IV Curve doesn’t display conductance decrease at extreme negative potentials.

(C) Kcv single-channel traces and single-channel opening events (enlarged) recorded with the two different solutions.

Slow gating

Kcv macro currents presented in fig. 12 are affected by at least another "slow gating" mechanism (fig. 15), which is responsible for closures in the range of msec, and which leads to a very low Single channel Open Probability (1 to 3%, fig. 25b): in the majority of the measurements Kcv spent most of the time in a closed conformation. Fig. 25b shows also that the Slow gating mechanism is slightly voltage dependent, as becomes obvious from a higher Open Probability at negative voltages.

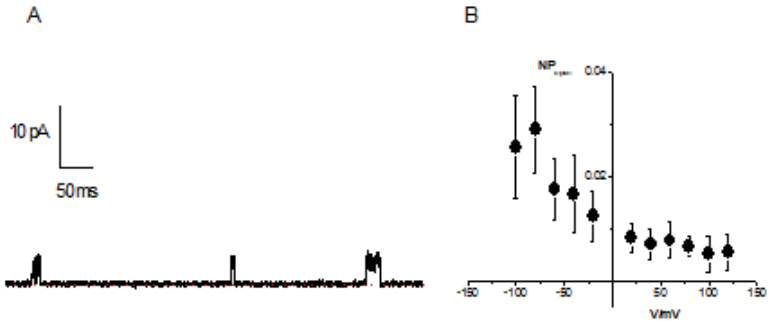

Fig 25:

(A) Kcv Single channel trace recorded at +40 mV.

(B) Voltage dependence of the Steady-state Open Probability.

The voltage dependence of this gating mechanism generates at negative voltages a slow increase of the Open Probability. In the experiment of fig. 26 the membrane potential was clamped at -60mV for one hour, and an increase of the Open Probability lasted for 45min. The time scale of this experiment is not comparable with that of the steady state Open Probability plotted in fig. 25b; however, we cannot exclude a relation between these data. On the basis of this knowledge, I tried to change the protocol used to record Kcv currents: the measurements used to calculate the steady state Open Probability of fig. 25b were done inverting the polarity of the membrane potential after every voltage step (i.e., -20mV, +20mV, -40mV, +40mV, ecc.), measuring for 30sec to 2min at each potential. On the contrary, in one other experiment (fig. 27), I recorded Kcv single-channel activity measuring before at all the negative potentials (i.e. -20 mV, -40mV, -60mV, ecc.), and then at all the positive potentials (i.e. +20mV, +40mV, +60mV, ecc.), measuring again for 30sec to 2min at each potential (continuous- activating or inactivating protocol). As result, the graph of fig. 27b has a similar shape to that of fig. 25b, but with a larger range of Open Probability values. I used this protocol just for one measurement, and a higher number of experiments will be necessary to confirm and better describe this phenomenon.

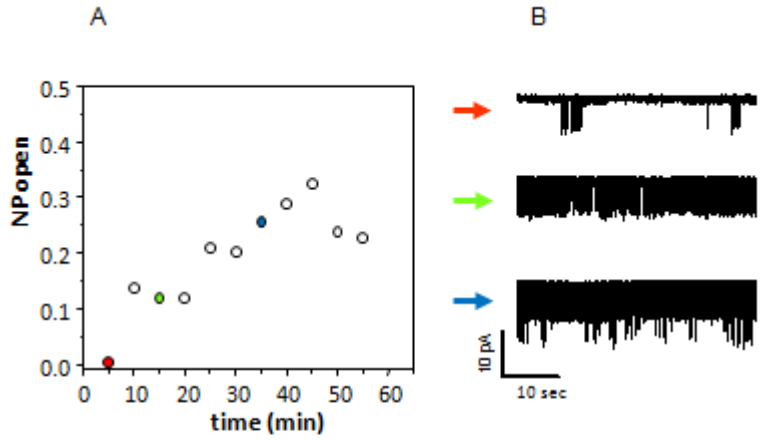

Fig 26: Kcv Open Probability increase during a 1 hour experiment at -60mV.

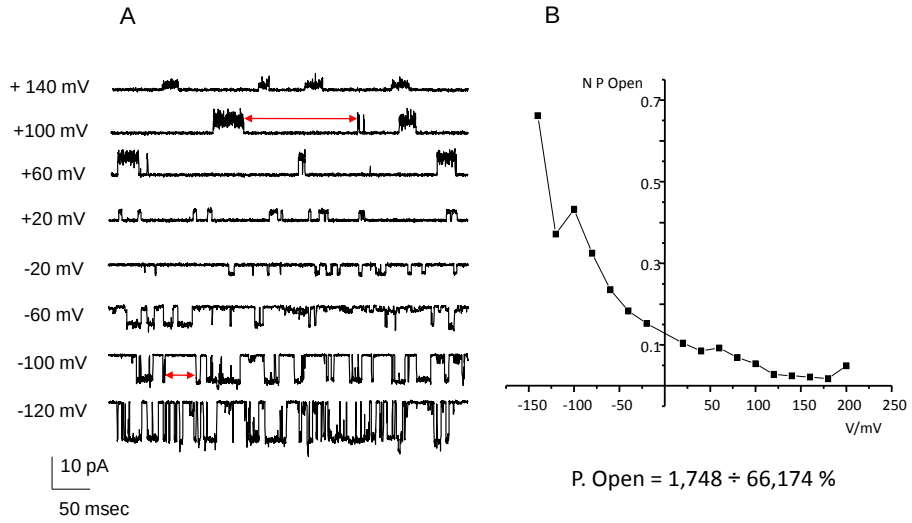

Fig 27:

(A) Single-channel traces at different membrane potentials recorded with a “continue- activating or inactivating protocol”. Red arrows show Slow gating closures at +100mV and -100mV.

(B) Open Probability from the same experiment , showing a strong voltage dependence.

With the goal of understanding the molecular reasons of such a mechanism of gating, we were looking for a mutant with a higher Open Probability. An increase of conductance at the macro current level, in comparison with wt conductance, can be due to a higher expression of a mutant channel, a higher Single channel Conductance, or an increased Open Probability. One of the Kcv mutants analyzed in our laboratory, Kcv P13A, display higher macro current conductance in both Xenopus oocytes and HEK cells (fig. 28), and was a good candidate for testing if the Slow gating mechanism is affected. Also Molecular Dynamic Simulation experiments supports the view that such a mutant has an altered gating mechanism, probably

located at the level of the cavity (fig. 29): the C-terminal portions of the second transmembrane domains can be close enough to narrow the way where K^+ ions pass through, in a similar manner to the "bundle crossing" mechanism described for KcsA (Introduction). In the mutant channel it seems that the N-terminal Slide-helix loses its interactions with the lipid membrane, imposing a higher flexibility of the second transmembrane domains, and therefore enlarging the tight K^+ ions passage.

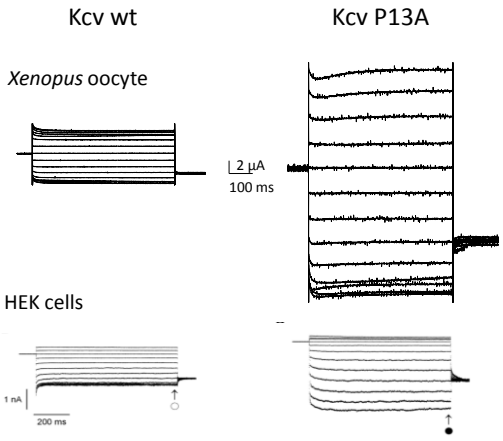

Fig 28: Kcv wt and Kcv P13A macro currents recorded in Xenopus oocytes and in HEK 293 cells. Kcv P13A macro currents display in both cases a current increase.

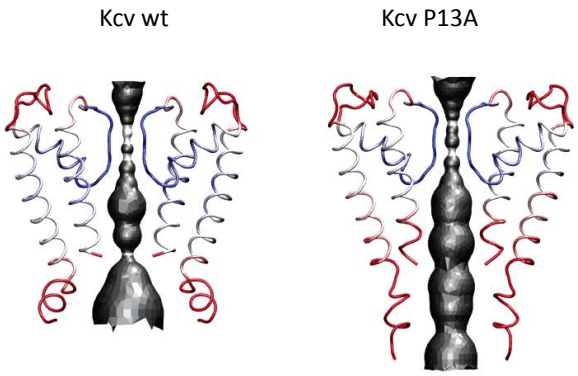

Fig 29: MD simulation of Kcv wt and Kcv P13A, showing a central electron density (of water molecules) higher for Kcv P13A.

Comparing Single channel traces, recorded with the same protocol and in the same conditions, we found that the mutant channel Kcv-P13A has a higher Single channel Open Probability at both positive and negative potentials in comparison with the wt channel. Single channel traces measured at +/-80mV are presented in fig. 30, from Kcv wt and Kcv-P13A; in this experiment the Open Probability at +80 mV pass from 1,1% for Kcv wt, to 10% for the mutant channel, and at -80 mV pass from 2,8% to 34%.

Thanks to the analysis of the changes induced with P13A mutation, we now have a better understanding of Kcv Slow gating mechanism. The comparison with other Kcv like K^+ channels, with a different Open Probability, will highlight new aspects and give new information on this topic.

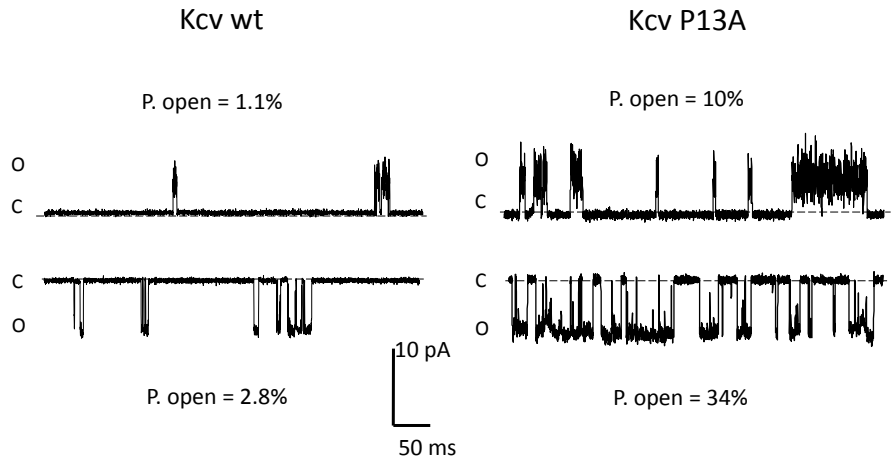

Fig 30: Kcv wt and Kcv P13A single-channel traces at +80 mV and -80 mV. P13A mutation affects the channel slow gating mechanism, increasing the Single channel Open probability.

Applications

A project presently running in our laboratory regards the possible technological applications of Kcv: the main idea is to fuse Kcv with other protein domains sensitive to specific environmental conditions. We hope that a structural change, induced in Kcv by the stimulus, will be able to modulate a gating mechanism, resulting thereby in different conductive properties.

In a previous project a construct was done fusing a Calmodulin domain to the C-terminal portion, and a M13 module (Calmodulin binding domain) to the N-terminal of Kcv, one of the main points for the control of Kcv Slow gate, with (fig. 31). TE-Voltage Clamp measurements have shown that an increase of the cytosolic calcium concentration in oocytes expressing such a chimera, results in a higher conductance of the inward Kcv currents (data not shown). During my PhD I have been measuring single channel activity from the same chimera in Inside-Out configuration, changing the calcium concentration of the internal solution. An appreciable variation of single-channel parameters was not detected; however, we cannot exclude an increase of single-channel Conductance or Open Probability, given the fact that I have obtained only a few recordings and that the variability seems extremely high.

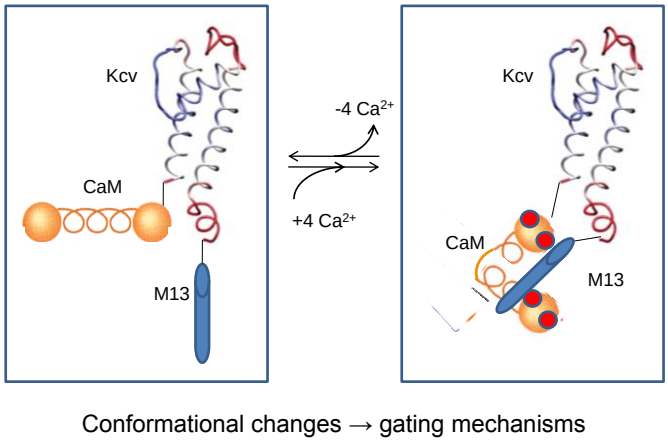

Fig 31: Possible usage of Kcv gating mechanism knowledge for biotechnological applications: fusion of Kcv with CaM and M13 modules.

Among the constructs planned to be tested in our laboratory, I can list a voltage-gated Kcv, a light-activated Kcv, and a ROS-gated Kcv. In one case the viral channel will be fused with the Voltage sensor domain of a VPS protein, a voltage-gated Phosphatase. Another construct will be done fusing Kcv with the Light Oxygen Voltage domain from the *Avena Sativa* phototropin, a blue light receptor. The ROS-gated Kcv will be done with the idea of induce conformational changes by the interaction of ROS with a Cysteine.

Discussion

PBCV-1 Kcv

The main result which emerges from the presented work is that a minimal K^+ channel as Kcv can display at least two different gating mechanisms, even if it lacks the domains that are considered responsible for K^+ channel gating such as the voltage sensor or the bundle crossing. This work is therefore interesting for the deeper understanding of the behavior of other K^+ channels too.

The analysis of Kcv macro currents had anticipated the finding that the two gating processes mentioned above are voltage-dependent. This becomes obvious from: the inactivation and activation kinetics at positive and negative voltages (fig. 12a), and the negative slope conductance of the IV Curve (fig. 12b). The analysis of single-channel traces allows the quantification of these mechanisms in terms of single-channel parameters. This enables their explanation from a molecular point of view.

Furthermore, Single channel IV Curves present the negative slope conductance at extreme voltages (fig. 13b), even when all the potential channel blockers are removed from the internal solution (fig. 14, red). This finding was unexpected at the beginning, as most of K^+ channels display an ohmic single-channel conductance. The conclusion was that the recorded decrease in single-channel conductance is an inherent property of Kcv. Thus a detailed analysis of Single channel traces becomes necessary.

Single-channel analysis revealed that the two voltage-dependent gating processes found in the macro currents can be assigned to a fast gating mechanism in a time scale of microseconds, and a slow one in a time scale of milliseconds (fig. 15). Their study required two different approaches.

Fast Gating

As described in the Results section, our analysis of Kcv Single channel currents reveals that fast flickering is the reason for the negative slope conductance of the IV Curve. At extreme potentials the recorded opening events are more noisy, and the average current level, plotted in the Single channel IV Curve, seems to decrease (fig. 16). β-distribution analysis (fig. 17a) revealed that the apparent conductance decrease is due to unresolved opening-closure events which occur with a frequency higher than the sampling frequency of the measuring apparatus (fig. 19b).

I will discuss the so-called depletion hypothesis (Schroeder I. and Hansen U.P., 2007, Abenavoli A. et al., 2009): the fast opening-closure events have been explained with an increasing instability of the Filter at extreme potentials, stronger at positive than at negative voltages (fig. 16); even if the same mechanism affects also the inward currents, it had been analyzed with β-distributions only at positive voltages as more evident at these voltages.

A strong support for the depletion theory, described in the Result section, comes from a comparison with results of crystal structure analysis: we have evidence that a higher K^+ concentration of the surrounding solution can better stabilize the Filter region of potassium channels (McKinnon et al., 2001). This is in agreement with the findings in fig. 19, showing that the Filter gets more stable at higher K^+ concentrations. The Ion depletion model (fig. 20) explains the higher instability at extreme voltages as the result of a stronger driving force that pushes ions from the Filter to the external solution more than their rate of refilling from the Cavity. A temporary absence of ions causes the Filter to collapse, generating fast closures and the fast flickering behavior. A higher potassium concentration of the internal solution is able to balance the two rates of exit and refilling of ions from and to the Filter, ensuring the presence of ions in this region, and therefore preventing its collapse.

As described in the Introduction, the Filter region of potassium channels coordinate potassium ions with four oxygen atoms per subunit, reproducing the environment that surrounds an hydrated ion solved in water. However, this region is not rigid; instead, some degree of flexibility has to be assumed, which depends on the number and the strength of interactions with the surrounding domains, like for example the Filter helix (Cordero-Morales et al., 2007). According to the results of fig. 19c, the Filter region of Kcv is more instable than that of MaxiK, as shown by the fact that the R factor (the ratio between the “true” and the “apparent” current value) is higher in Kcv than in MaxiK. Inspecting the IV curves of other K^+ channels indicates that Kcv is affected by a higher instability in comparison also with many other potassium channels. This can be deduced on the fact that Kcv lacks additional domains that can stabilize the protein conformation in the membrane.

In the experiments of fig. 21, 300mM KCl is able to partly stabilize Kcv Filter: the average conductance level doesn’t decrease at extreme voltages, even if some opening events still display a high flickering

behavior. Thus it might be desirable to use even higher KCl concentrations. Unfortunately, measurements with higher K^+ concentration are not feasible because of a higher instability of the Patch and the resulting background noise of the recorded traces.

An interesting feature of the gating behavior is a variability of the voltage-dependence: in the most of the experiments Kcv displayed stronger fast flickering at positive than at negative voltages (fig. 16). However, in some cases we found a more pronounced flickering at negative voltages as shown in the experiment of fig. 23. We cannot exclude an inverted insertion of Kcv in the membrane, as it was found for other membrane proteins (Dunlop J., et al., 1995; Marques E.J., 2004); however, the most likely explanation is that a different membrane composition can affect channel properties, as the two different kinds of voltage-dependencies were mostly found in different batches of oocyte. For example membrane components such as cholesterol or other protein can interact with the channel affecting its activity (Dart C., 2010; Galan C. et al., 2010).

As the fast flickering of the outward currents, also that of the inward currents was modulated by increasing the potassium concentration, in that case, of the external solution (fig. 24). The effect on fast gating was different in comparison with that found when outward currents were modulated: the opening events recorded with high potassium display an homogeneous behavior characterized by a decreased noise to signal ratio. On the contrary, the same experiment leads to an heterogeneous fast flickering behavior of the opening events when outward currents were modulated. This finding supports the view that a different orientation of the channel in the membrane is probably not responsible for the observed opposite behavior of Kcv in different batches of oocytes.

Slow Gating

The results of my study on slow gating in Kcv can be compared with the findings in other K^+ channels. For instance in KcsA a gating mechanism was found at the level of the second transmembrane domains, known as bundle crossing (Introduction). At a first glance, it does not seem to be possible to have such a bundle crossing in Kcv, as the second transmembrane domains are too short to cross (19aa). On the other hand, Molecular Dynamic Simulation show that the α-helixes can come close enough to narrow the way where K^+ ions pass through (fig. 29, Kcv wt). This would give a possible explication of the low Open Probability displayed by Kcv Single channel traces (fig. 25a).

The second feature of slow gating in Kcv is its voltage-dependence, found in macro currents (fig. 12) as in single-channel recordings: the single-channel Open Probability is higher at negative voltages (fig. 25b). Such a voltage dependence could be due to changes in the number and strength of interactions between the first and the second transmembrane domain or between the lipids and the Cytosolic Slide helix (Hertel B., et al., 2006); these changes could affect the flexibility of the second transmembrane domains, thus creating a mechanism similar to that of bundle crossing in KcsA.

In addition to the mechanism similar to bundle crossing, also a slow adaptation mechanism seems to occur in Kcv. This could explain the stronger voltage dependence of the traces presented in fig. 27: this is the only experiment where I did not apply command potentials with alternating polarity. Instead , a series of negative potentials was followed by a series of positive potentials (see Results, *Slow gating*). Avoiding the switching between positive and negative potential during a series of voltage steps of increasing magnitude, a putative activation process (at negative potentials) or inactivation process (at positive potentials) could accumulate. This protocol resulted in a stronger gap between Open Probability at positive and negative voltages. This finding will be further analyzed in new experiments.

Surprisingly, the activation induced at negative voltages seems not saturate even after 45min, as shown in the experiment of fig. 26, where the Patch was clamped at -60mV for 1 hour. That was a single experiment that needs to be confirmed by future measurements; however, it gives the idea of a very slow activating mechanism, that could, differently from our first interpretation, be independent from the previously described mechanism similar to bundle crossing.

This interpretation is supported by the findings related to the Kcv mutant P13A. Here the freedom of movement of the second transmembrane domains, and therefore of the putative bundle crossing, supposed to be at the basis of the Open Probability voltage dependence, is modified (fig. 29). As a consequence, the mutant channel display a higher Open probability, but with a similar voltage dependence (found also for all potentials from -120mV to +100mV, data not shown).

The main conclusion is that Kcv can have a very similar slow gating mechanism; even though it lacks the same bundle crossing as found in KcsA because of its minimal structure. The results presented in this thesis

give rise to the idea that some kind of primitive bundle crossing modulates Kcv gating properties. Such a property of Kcv is in agreement with the tendency of viruses to compact all their genetic information in a DNA or RNA molecule as small as possible, generating proteins with the smallest length, but still with many of the important properties described for similar proteins from major organisms.

It doesn't surprise in that view that Kcv, thanks to its minimalistic structure, is considered a good model for study of the properties of all potassium channels.

Applications

There is growing interest in biotechnological applications with the prospective of linking the knowledge of properties and functions of studied proteins with the increasing demand of more sensitive and specific devices. For instance, some of these instruments should be able to quantify the concentration of a specific substrate, or detect the presence of a physical phenomena. The usage of a protein as sensor (biosensor) can enable a higher sensitivity to environmental stimuli.

Kcv, thanks to its minimalistic structure and on the basis of the knowledge we have on its functionality, is a good candidate for this kind of biotechnological application. This prospective is in progress and different constructs, maybe useful as component of a biosensor, have been tested in our laboratory.

The experiments performed on the Kcv chimera, obtained by the fusion of Kcv with a Calmodin and the M13 domain (fig. 31), didn't show a convincing effect of intracellular calcium on the activity of the channel.

We hope in the future that new constructs will display a stronger sensitivity to environmental factors, helping thereby the development of biosensors, and providing a new point of view important for the understanding of potassium channel properties.

Influenza A PB1-F2

Materials and Methods

Influenza A PB1-F2

1) In vitro protein production

In order to synthesize the full-length version of the swine Flu PB1-F2 peptide, its original encoding sequence was mutated substituting the first two stop messages into the sequences encoding a Serine and a Tryptophan respectively. These are considered to be the most probable amino acids that could arise from viral spontaneous mutations of the wt sequence.

The new peptide (aPB1-f2sf) was in vitro synthesized, and the dehydrated protein was stored at -80°C; we can therefore assume that no contaminations were present in the protein samples. Before reconstituting into artificial lipid bilayer, 1 mg/ml aliquots were prepared, dissolving the protein in water, and stored at -20°C.

2) Protein reconstitution and electrophysiological measurements

The artificial lipid bilayer chamber is composed by a cis- and a trans- compartment, separated by a Teflon foil, where a hole is made for the artificial membrane reconstitution. A 0.4 mg/ml solution of a-phosphatidylcholine (type IV-S >= 30 % TLC; Sigma-Aldrich (Steinheim, Germany)) in n-decane (Carl Roth, Karlsruhe, Germany) is released on the Teflon foil hole and washed with the experimental solution, after at least one hour for complete n-decane evaporation, until formation of a lipid bilayer. A 30 min control measurement is done before reconstituting the protein, in order to exclude any possible contamination of the bilayer chamber, or experimental solutions. 0,5 to 3 µl of the 1mg/ml protein aliquots were added in the 2,5 ml experimental solutions (final concentrations: 0,2 to 1,2 ng/µl, or 50 to 300 nM), and the solution was mixed until channels signals could be recorded.

The measurements were done with symmetrical KCl solutions (500mM KCl, 10mM Mops/Tris pH7) or in non-symmetrical conditions with the same KCl solution in the trans- compartment, and a NaCl solution (500mM NaCl, 10mM Mops/Tris pH7) in the cis- compartment . The Ag/AgCl electrode of in the trans compartment was directly connected to the head stage of a current amplifier (EPC 7, List, Darmstadt, Germany); the electrode in the cis-compartment was connected to the ground. At positive potentials the electrode in the trans-compartment was positive and the electrode in the cis-compartment negative. In order to prevent surface-potential effects both electrodes were connected with the bath solution via an agar bridge (2% agarose in 2 M KCl). Currents were recorded and stored by an analog/digital converter (LIH 1600, HEKA electronics, Germany) at 4 KHz after low pass filtering at 1 KHz. Data analysis were performed by Patchmaster-Software (HEKA electronics).

3) Cell culture and macro currents measurements

R28 cells (rat Retinal precursor cells) were chosen for Port-a-Patch measurements because of the quality of their seals in comparison with HEK 294 cells. They were incubated at 37°C until reaching 80% confluence, and isolated with 1ml Trypsine/EDTA. The reaction was stopped with 1ml of "R28 media" (DMEM + stable L-Glu, 10% FCS, 1% Penicillin/Streptomycin), and cells were centrifuged and suspended in 250µl of the experimental external solution(4mM KCl, 140mM NaCl, 1mM $MgCl_2$, 2mM $CaCl_2$, 5mM D-Glucose monohydrate, 10mM Hepes /NaOH pH 7.4).

For Port-a-Patch experiments borosilicate glass chips were used, where 5µl of internal solution (50mM KCl, 10mM NaCl, 60mM K-Fluoride, 20mM EGTA, 10mM Hepes /KOH, pH 7.2), and 5µl of external solution (connected to the measuring electrode, and ground electrode respectively) were added on the two opposite sides of a 5µm hole. The provided Nanion program automatically apply a negative pressure that attracts cells from the external solution to the hole; pressure is stopped when the measured resistance reaches about 1GΩ because of the seal formation. In order to improve the seal, an enhancing solution was added at the external side, with a higher calcium concentration (80mM NaCl, 3mM KCl, 10mM $MgCl_2$, 35mM $CaCl_2$, 10mM Hepes /NaOH pH 7.4). Once the recording apparatus automatically passed from cell-attached to whole-cell configuration, suspended cells and enhancing solution were washed in order to have 25µl of fresh external solution on the external side.

After measuring R28 endogenous currents, aPB1-F2sf was added to the external solution at 1µM, 500nM, 100nM and 10nM concentration. Whole-cell currents were measured at 10KHz, and filtered with a 2KHz cutting frequency; voltage protocols were: i) a 400msec holding potential of -60mV, ii) 1200msec, -20mV voltage steps from +80 to -120mV, iii) 400msec tail voltage of -80mV. PatchMaster and FitMaster were used to record currents and analyze data respectively.

The same protocol was used to measure aPB1-F2sf activity in HEK-294 cells, adding the peptide at 1µM concentration.

4) Microfluorimeter essay

R28 cells were grown following the same procedure described for macro currents measurements, and incubated with 1µM fluorescence dye Fluo-4 (Invitrogen) for 25min. After washing with the same external solution used for macro currents measurements, another 30min were waited to allow intracellular deesterification of the fluorescent compound.

Changes in the cytosolic concentration of Ca^{2+} were measured as a function of the fluorescence signal: Fluo-4 was excitated with 294nm light, resulting in an emitted light at 516nm. Cell fluorescence images were collected by a Fluorescence Microscopy every 2-3min.

The viral peptide aPB1-F2sf was added at 1µM and 10µM concentration, while Ionomycin was added at only 1µM concentration.

Results

PB1-F2

During my PhD I have been working, in collaboration with Professor Gerhard Thiel (TU Darmstadt, Germany), in order to analyze the properties of the swine Flu Influenza virus encoded peptide PB1-F2.

PB1-F2 is a short protein of about 90 amino acids expressed by many influenza A viruses (IVA). Its gene derives from an alternative open reading frame of the sequence encoding for the viral Polimerase PB1, and the peptide was shown to confer a higher pathogenicity to Influenza viruses (Conenello G.M., et al., 2007). The swine Flu virus, which emerged in 2009/2010, does not code for a full length protein because the gene comprises three stop codons which prevent the synthesis of the channel forming c-terminal α-helix (Fig. 32A). The absence of a full length PB1-F2 protein is probably at the basis of the relatively low virulence of the swine Flu IAV (Hai R., et al., 2010).

To test whether future mutations of these stop codons into codons for amino acids would generate an active channel forming peptide, a mutant sequence was estimated in which the first two stop messages were converted into the amino acids which most likely occur by a mutation in the respective stop codons. The resulting protein is similar to the channel forming PB1-F2 peptides from the Perto Rico isolate of influenza H1N1 ($PB1\text{-}F2_{pr}$) (compared with Henkel et al. 2010). An alignment of the PB1-F2 protein from the Puerto Rico H1N1 isolate and the full length PB1-F2 from the swine Flu virus, which is expected to emerge after mutations of the first two stop codons, is shown in Fig. 32B (Prof. U. Schubert, Uni. Erlangen, Germany). Since the third stop codon is at the end of the C-terminus it was anticipated that the two remaining downstream amino acids may not be relevant for function and that already a mutation of the two most N-terminal stop codons might be sufficient to produce a functional peptide. This anticipated PB1-F2 peptide (now called aPB1-F2sf) was synthetically made (Henklein P. et al., 2005) and tested for its channel forming activity.

I studied the characteristics of aPB1-F2sf using three different techniques: the planar lipid bilayer technique, electrophysiological measurements of macro currents with the Port-a-Patch system, and Fluorescence Microscopy.

Met E Q E Q D T P W T Q **Ser** T E H T N T Q K R E S G R Q T Q R L V H P S S T R L
Met D H Y L R I **Met** N Q V G **Met** H K Q T V F **Trp** R L W L S L K N P T R E Y L R I H A
L K Q W K L F N K Q G **Stop** I N **Stop**

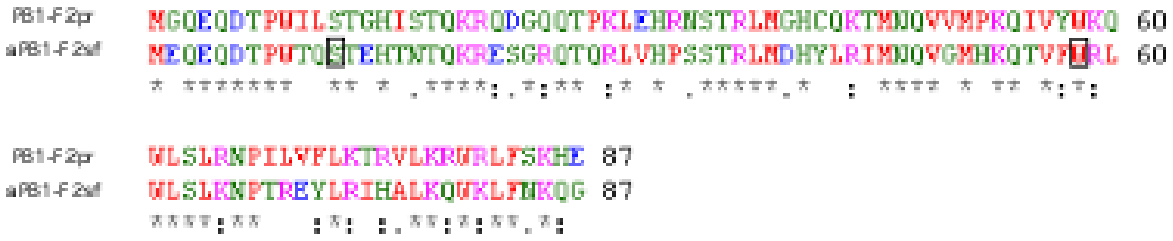

Fig. 32. PB1-F2 proteins from swine flu and from influenza A virus (Puerto Rico/8/34(H1N1) isolate.

A: The H1N1 type swine flu virus of 2009/2010 does not code for a full-length PB1-F2. The peptide sequence (PB1-F2sf) is interrupted by three stop codons.

B: The anticipated protein structure of full length PB1-F2 from swine flu virus (aPB1-F2sf) can be estimated by assuming a minimum of mutations of the stop codons to code for amino acids. The anticipated full-length aPB1-F2sf protein expected in future emerging viruses, in which the first two stop codons are replaced by a Serine and a Tryptophane respectively (indicated by boxes) is aligned with the channel forming PB1-F2 protein from Puerto Rico H1N1 strain (PB1-F2pr). Note the high degree of identity (+) and homology (:,.) between the two proteins.

Reconstitution of aPB1-F2sf in planar Lipid bilayers

In the presented work, I show for the first time single channel traces from the swine Flu Influenza virus encoded aPB1-F2sf mutated peptide.

The reconstitution of the synthetic peptide in planar lipid bilayers shows that the protein indeed generates canonical channel fluctuations in artificial lipid bilayers (Fig. 33). As other Pb1-F2 peptides, encoded by different influenza viral strains (Henkel et al. 2010), also aPB1-F2sf is able to generate different conductance levels within the same window of membrane potentials. The recorded current levels are probably related to the number of subunits that interact to form a channel: the larger the number of subunits, the larger will be the size of the internal pore, and hence the conductance level.

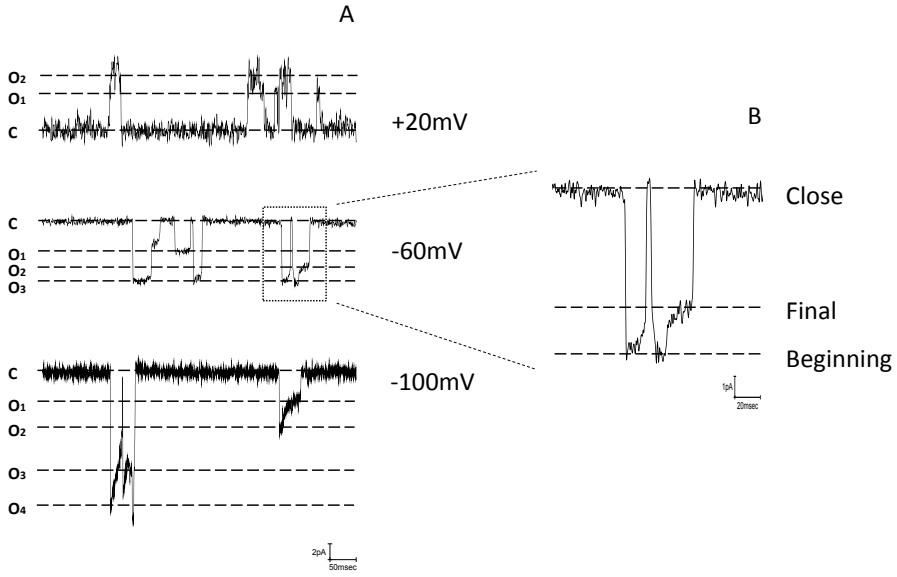

Fig. 33: aPB1-F2 generates channel fluctuations in planar lipid bilayers. 500msec long traces with single channel fluctuations generated by aPB1-F2sf in planar lipid bilayer at different potentials. Close and Open state are marked (C, O). Enlargement of an opening event at -60mV, where the beginning and final current level is shown.

At extreme potentials (e.g. +/-100 mV) single channel opening event occurred more frequently, and it is possible to find new conductance levels with higher values (Fig. 33a). I have not analyzed this phenomenon, but we can speculate that at extreme voltages the interaction between subunits is promoted; on the contrary, it is probably not due to a voltage dependent mechanism of gating, as PB1-F2 peptides form non-specific channels, which lack any kind of voltage sensor. Occasionally it was possible to observe also a decrease in conductance during an opening event (Fig. 33b). Similar observations were made

in previous measurements with other PB1-F2 proteins (Henkel et al. 2010). These data underscore the fact that the different conductance levels are not generated by different independent proteins. The data are more consistent with the idea that a single channel forming complex has different conductances; in the case of the data shown in Fig. 33b we may speculate that one or more subunits might have dissociated from the conducting channel.

The two most frequently occurring conductance levels are plotted against the membrane potential (Fig. 34a, g1 and g2). A linear fit through the data shows that the channel has an ohmic behavior and the two conductances have a value of 64,83 ±1,02 pS and 223,87 ±2,54 pS respectively. In Fig. 34b single channel conductances generated by PB1-F2 peptides from three other Influenza A virus strains are plotted together with a linear fit (Henkel et al. 2010); in the same graph the unitary conductance levels from aPB1-F2sf are plotted (red squares), highlighting the similar behavior of the four peptides.

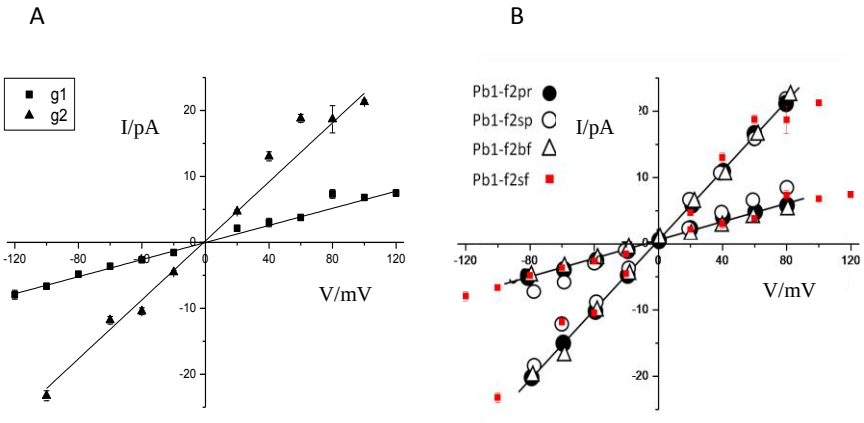

Fig. 34

A) Single channel IV Curve from aPB1-F2sf. The two main conductance levels (g1 and g2) and their linear fit are shown. The two conducatnaces are 64,83 ±1,02 pS and 223,87 ±2,54 pS respectively.

B) Single channel IV Curves from PB1-F2 from three different Influenza virus strains (PB1-F2pr, PB1-F2sp and PB1-F2bf; for nomenclature see Henkel et al. 2010). Two conductance levels and their linear fit are shown; in the same graph g1 and g2 from aPB1-F2sf are reported (red).

These data show that aPB1-F2sf, once mutated in two Stop codons, is able to insert in lipid membrane and generate functional channels with characteristics similar to PB1-F2 from other viral strains. We can therefore hypothesize that, with two similar mutations, the swine Flu Influenza virus can display in the future a higher pathogenicity.

Macroscopic membrane currents

The functional role of PB1-F2 in virulence is not yet fully understood: expression studies revealed that the peptide is found in the mitochondria of infected cells (Gibbs J.S., et al., 2003), where it is thought to execute its pro-apoptotic activity, generating an ion conductance which destabilizes the mitochondrial membrane (Chanturiya A.N., et al., 2004). It is less clear whether the viral protein also has a role in the cytosol or in the nucleus of infected cells, where it can also be observed albeit at a lower concentration (Chen W., et al., 2001; Gibbs J.S., al., 2003). After analyzing aPB1-F2sf single channel behavior, I have in the next step also been examining whether such a peptide is able to insert into the plasma membrane of mammalian cells. This could for example become relevant when a PB1-F2 expressing cell is dying and releasing its content (Chen W., et al., 2001). To examine the effect of aPB1-F2sf on the plasma membrane I measured the macroscopic current activity of R28 cells (Retinal precursor rat cells) in the whole-cell configuration, before and after the addition of aPB1-F2sf at different concentrations to the external medium.

The endogenous currents of R28 cells are characterized by a weak inactivation at negative potentials, and an appreciable time dependent activation at positive voltages (Fig. 35a, control). Experiments in order to analyze the selectivity of outward currents has not been done; we estimate however that such a behavior is probably due to the presence of outward rectifying potassium channel in the membrane of these cells. Under control conditions, the membrane currents in R28 cells tended to decrease, after achieving the whole-cell configuration, until reaching a stable conductance level. This phenomenon could result from a rundown effect, generated by a decreasing ATP-dependent potassium channels activity (Mauerer U.R., et al., 1998; Pian P., et al., 2006). But in addition to ATP also other relevant control factors might be washed out from the cytoplasm in the whole cell configuration. It is also possible that the constant negative pressure, which is applied from the measuring apparatus could contribute to this phenomenon.

Once aPB1-F2sf was added to the external medium, an increase in both inward and outward currents was generated (Fig. 35a, +PB1-F2 1µM). This effect was specific for the aPB1-F2sf peptide since the addition of the boiled peptide (96°C, 15min) had no perceivable effect on the currents (Fig. 35a, + boiled PP1-F2 1µM). Only after adding the active aPB1-F2sf peptide the currents increased over the entire voltage range.

The results of these experiments show that aPB1-F2sf is able to insert into the plasma membrane of mammalian cells, where it generates a current increase. A detailed analysis should uncover which mechanism generates this kind of effect.

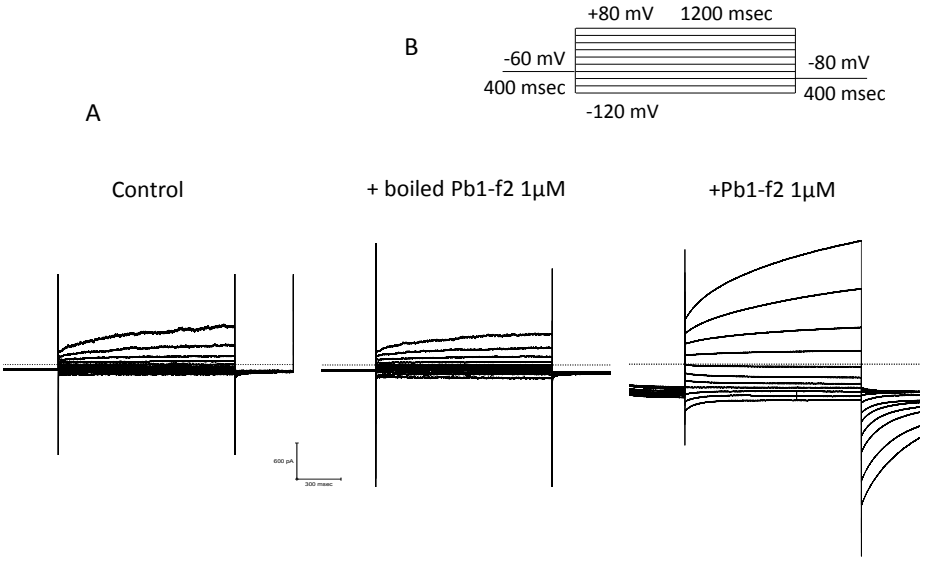

Fig. 35:

A) Macroscopic currents of R28 cells recorded in control conditions and after the addition of boiled and un-boiled aPB1-F2sf at 1µM to the external solution. B) Voltage Clamp Protocol.

To examine the concentration dependency of the aPB1-F2sf effect, cells were challenged with different concentrations of the peptide. The data in Fig. 36 show that the stimulating effect on currents increases with higher aPB1-F2sf concentrations. Fig. 36 shows exemplary current traces measured at test pulses from -60mV to +80mV and a post pulse to -80mV, before (black) and after (red) aPB1-F2sf addition to the external medium. It is possible to appreciate that the induced increase in currents decreases with a decrease in the peptide concentration from PB1-F2 1µM to PB1-F2 10nM. At the lowest concentration we even measured a tiny current decrease with respect to the control experiment (black). The latter is probably explainable with the usual reduction of the endogenous currents which probably masks a possible small aPB1-F2sf induced current increase (Fig. 36, 10nM).

The time required for aPB1-F2sf to increase the currents in R28 cells can be fast. Fig. 37 shows an exemplary experiments where 1µM aPB1-F2sf was added to the bath medium of R28 cells. Before addition of the viral peptide the current level at +80mV was rather stable and showed only a small decrease. The addition of boiled aPB1-F2sf protein generated no appreciable change in current. After addition of 1µM active aPB1-F2sf the current increased dramatically. In the present case already the first measurement taken after the addition of the peptide revealed an elevated current compared to the control. The same fast response to aPB1-F2sf was observed in similar experiments meaning that the cellular response to the peptide is within the first 2 minutes of treatment.

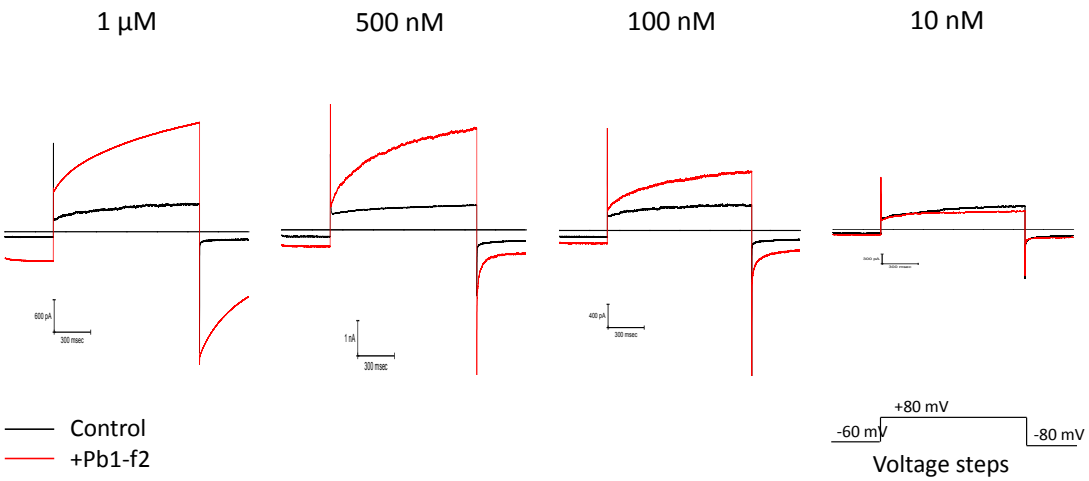

Fig. 36: Macroscopic current response of a R28 cell from holding voltage to +80 mV before (black) and after (red) adding aPB1-F2sf at different concentrations to the bath medium

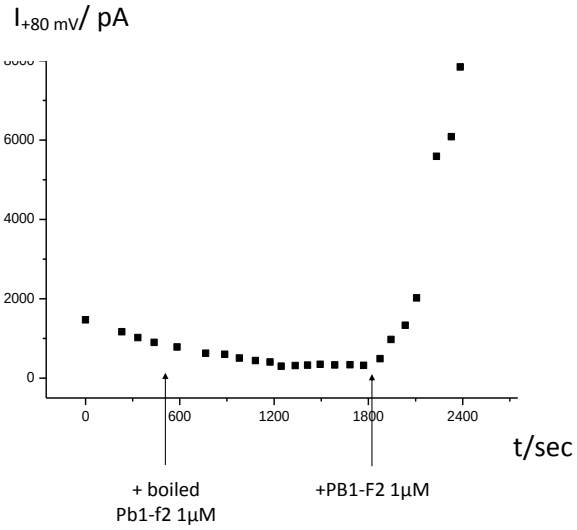

Fig. 37: +80mV Steady State Current level during the experiment. 1µM aPB1-F2sf was added in the external solution.

For the further analysis of the aPB1-F2sf effect on R28 macro currents, I separated the effect of the viral peptide on the instantaneous and the time dependent conductance.

The increase of the instantaneous current, induced after the addition of 1µM aPB1-F2sf, is shown in Fig. 38. The data reveal that the peptide causes a ca. 3 fold increase in the linear conductance of the instantaneously activating current. The fact that aPB1-F2sf is generating channel conductance already by itself in membranes suggests that this rise in conductance reflects the direct activity of aPB1-F2sf channels inserted in the cell membrane.

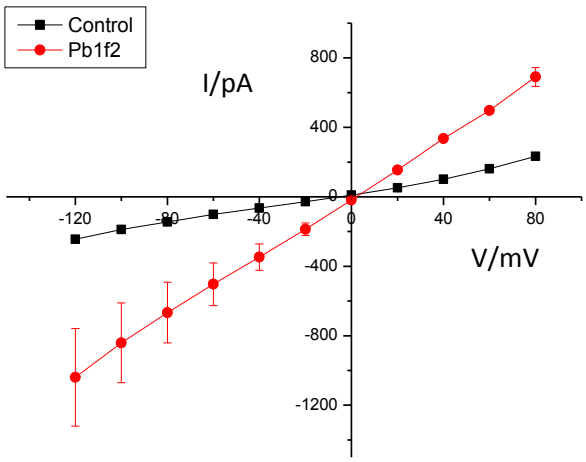

Fig. 38: I/V relation of instantaneous activating current in HEK293 cells before (black) and after (red) addition of aPB1-F2sf 1µM in the external medium.

Also the time dependent current increases after addition of aPB1-F2sf to the medium: in Fig. 39a the macroscopic currents from one cell evoked by a voltage step from 0mV to +80 mV are shown. The current traces were recorded before (black) and after (red) addition of aPB1-F2sf. The data are plotted such that the time dependent currents start at the same origin. The difference between the currents at the end of the voltage step to +80 mV was evaluated as measure for the time dependent current, and was plotted for all the positive voltages (Fig. 39b). The comparison of the current values recorded before and after addition of aPB1-F2sf shows that the peptide generates a strong increase in this time dependent outward current. Such an increase of the time dependent current following the addition of aPB1-F2sf to the external medium could be due to a scaling up of the outward rectifying channels or by a change in the voltage dependency of these channels.

In order to discriminate between these two hypotheses, I compared the kinetics of the current responses from Fig. 39a by normalizing them to the same ordinate. Fig. 40a shows that the aPB1-F2sf generated increase in conductance has no appreciable effect on the shape of the endogenous currents kinetics. The result of this analysis implies that aPB1-F2sf has no appreciable effect on the kinetics of the endogenous outward rectifier. This conclusion is supported by the comparison of the activation curves obtained before and after challenging cells with aPB1-F2sf. When relative open probability curves, which were derived from the Tails currents, were normalized to the same ordinate (Fig. 40b) the curves were not different for currents recorded before or after addition of aPB1-F2sf. This demonstrates that the voltage dependency of the endogenous outward rectifier is not affected. Collectively this means that the peptide results in a scaling up of either the number of active channels or in an elevated conductance of the single channel amplitude of endogenous channels.

The origin of the aPB1-F2sf-induced increase in conductance of the endogenous outward rectifier is not known. One possibility is that aPB1-F2sf generates pores in the membrane and that these pores carry Ca^{2+} inside the cell (see below). Such an elevation of Ca^{2+} could result in an activation of Ca^{2+} sensitive channels in the membrane of cells.

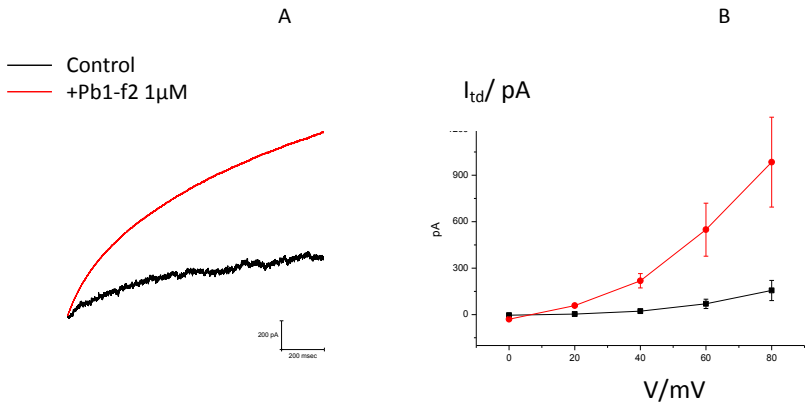

Fig. 39: Addition of aPB1-F2sf at 1µM to the external medium generates an increase in the endogenous slow outward rectifier in R28 cell.

(A) Time dependent macroscopic current responses to voltage step from -60mV to +80mV before (black) and 6min after (red) adding 1 µM aPB1-F2sf to bath medium. The current responses were scaled to the onset of the slow rise in current.

(B) IV relations of slow activating outward rectifier before and after treatment of cells with 1µM aPB1-F2sf. The currents are the means (+/- standard deviation; n: 3 different cells); they report the difference between the current value at the end of the voltage step to a positive voltage minus the current at the onset of the slow current at the respective voltage.

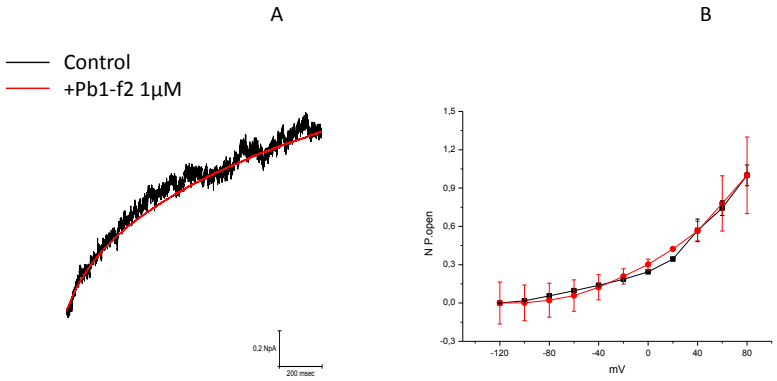

Fig. 40: Kinetics of macroscopic current responses to test pulse from -60mV to +80mV before and after addition of aPB1-F2sf at 1µM.

(A) Time dependent Macro currents at +80mV, scaled on the same beginning and final current levels.

(B) Normalized relative open probability as a function of voltage before (black) and after (red) addition of aPB1-F2. Data are mean values +/- sd of n= 3 measurements.

In a further step we addressed the question whether the aPB1-F2sf-induced rise in instantaneous and the

time dependent current was caused by the same or two different mechanisms. Our working hypothesis was that the increase in instantaneous current might be explained directly by aPB1-F2sf channel activity, while the effect on the time dependent currents might be the result of an indirect way of action. Further below we speculate that the latter could be the results from a MinK-like behavior of the viral peptide. MinK proteins are small proteins with a single transmembrane domain, which interact with K^+ channels and affect their performance (Barhanin J., et al., 1996; Sanguinetti M.C. et al. 1996). Pb1-F2 peptides display indeed some characteristics in common with MinK subunits: they are single transmembrane domains with charged amino acids, and they were found to interact with other membrane proteins like ANT3 and VDAC1 in the internal and external Mitochondrial membrane respectively (Zamarin et al., 2005).

The percentage of aPB1-F2sf stimulated increase in currents was plotted as a function of the aPB1-f2sf concentration for the two different current components (e.g. instantaneous and slow activating), and the deriving graph was fitted with a Michaelis-Menten equation (Fig. 41). The $K_{1/2}$ values resulted to be 29.95 ± 9.92 for instantaneous currents, and 73.46 ± 30.11 for time dependent currents. These values are affected by large errors; hence the difference in the apparent $K_{1/2}$ values is not significantly different. Hence, we cannot conclude on the bases of the does response relations that two different mechanisms are at the bases of the stimulation of the instantaneous and time dependent currents.

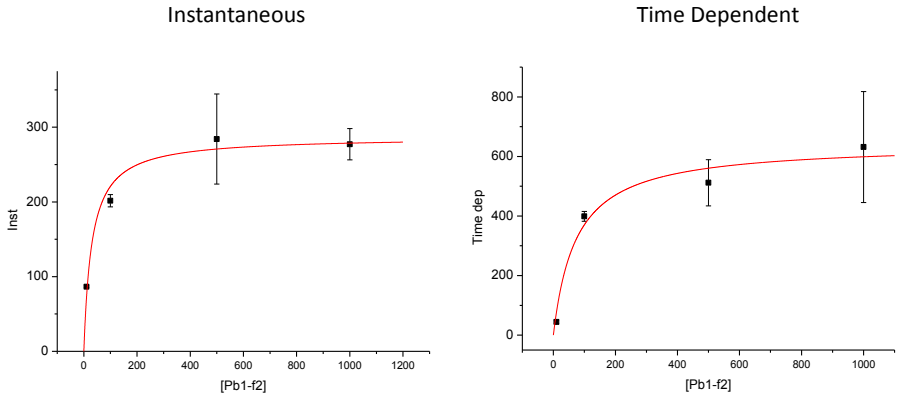

K_m = 29.95 ± 9.92 V_{max} = 287.03 ± 15.94

K_m = 73.46 ± 30.11 V_{max} = 642.93 ± 55.29

Fig. 41: Percentage increase of Instantaneous (left) and Time dependent (right) currents at +80 mV after addition in the external medium of aPB1-F2sf at different concentrations.

A control was needed in order to verify whether the aPB1-F2sf generated increase in membrane currents was a genuine characteristic of the viral peptide or specific for the type of cell in which the peptide was tested. For this purpose, aPB1-F2sf was added at 1 µM to the experimental external solution of HEK 293 cells. Also in this case the viral peptide increased the membrane currents albeit with some differences: the macroscopic current responses of a HEK293 cells to a standard voltage protocol in Fig. 42 suggest that the main contribution to the current increase results from Instantaneous activating currents; the time dependent outward rectifier seems not to be dramatically affected; the IV curves in Fig. 43 demonstrate indeed that the relative increase of the instantaneous current is stronger than that of the time dependent current; in this respect the data are different from the effect found in R28 cells. This result suggest that aPB1-F2sf interferes in a genuine way with the plasma membrane of cells. The alteration of individual currents however can be cell specific. It may be speculated here that the insertion into the membrane of HEK 293 cells is more efficient than in R28 cells; on the other hand the endogenous outward rectifier in HEK 293 cells seems to display a weaker sensitivity to the viral peptide. This overall difference in cell type specific response to aPB1-F2sf was confirmed in experiments in which the viral peptide was added at a concentration of 500nM to the bath medium of HEK 293 cells. Also in this case the measurements revealed mostly an increase in instantaneous activating current (data not shown).

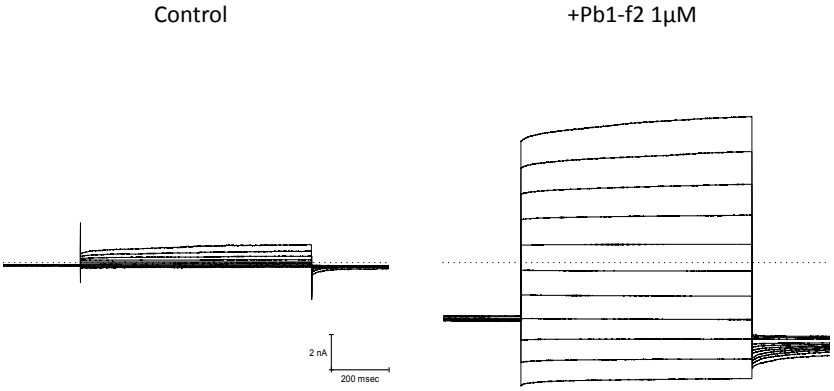

Fig. 42: Current response of HEK293 cell to standard clamp protocol before (left panel) and $ min after addition of 1 µM aPB1-F2 to the bath medium.

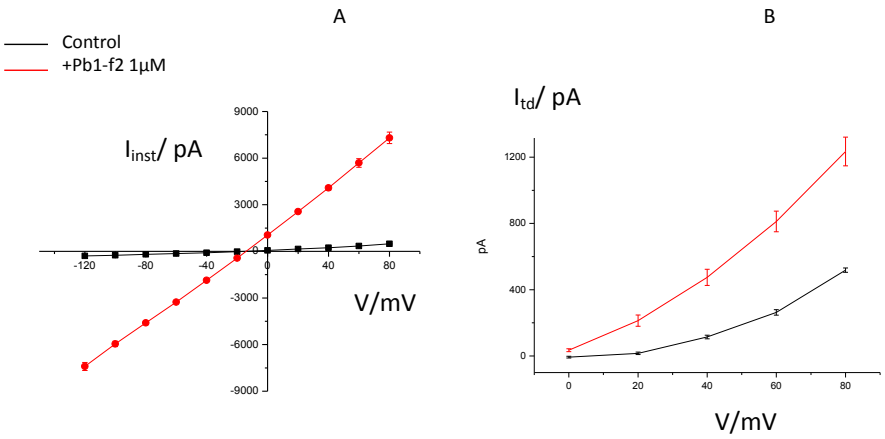

Fig. 43: I/V relation of instantaneous (left panel) and time dependent currents (right panel) before (black) and after (red) addition of 1µM aPB1-F2sf at to the external medium. The data are mean +/- standard deviation of 3 measurements.

Fluorescence Microscopy

Many signals are used in cells in order to transmit environmental changes, to induce a modification of their behavior, or to communicate with other cells. The cytosolic Ca^{2+} concentration often is a crucial parameter in the transmission of these physiological signals (Smaili S, et al., 2009); in many cases the elevation of Ca^{2+} results in a modification of Ca^{2+} sensitive ion channels. In the context of the present experiments we were interested to examine whether the activity of aPB1-F2sf is causing an increase in cytosolic Ca^{2+}. This is a reasonable assumption because previous work had shown that PB1-F2 generates channel activity in planar lipid bilayers with a permeability to Ca^{2+} (Henkel et al., 2010).

For this purpose we performed microfluorimetic measurements on R28 cells loaded with the Calcium sensitive fluorescent indicator Fluo-4-AM. This dye is an uncharged molecule with an ester group and can freely permeate cell membranes. Once inside the cell, the lipophilic groups are cleaved by nonspecific esterases, resulting in a charged form of the dye that remains in the cytosol, and binds Ca^{2+} ions. Binding of the dye to Ca^{2+} results in a concentration dependent increase in light emission at 516nm when excited at 494nm; the fluorescence intensity will hence be proportional to the concentration of cytosolic free Ca^{2+} (Invitrogen).

In a first experiment, R28 cells where treated with 1µM aPB1-F2sf (Fig. 44) but an appreciable change in fluorescence was not detected over a period of about 20min. To test the general responsiveness of the system, the same cells were then challenged with 1 µM Ionomycin. As expected this resulted in a strong increase in the fluorescence of the Ca^{2+} sensor.

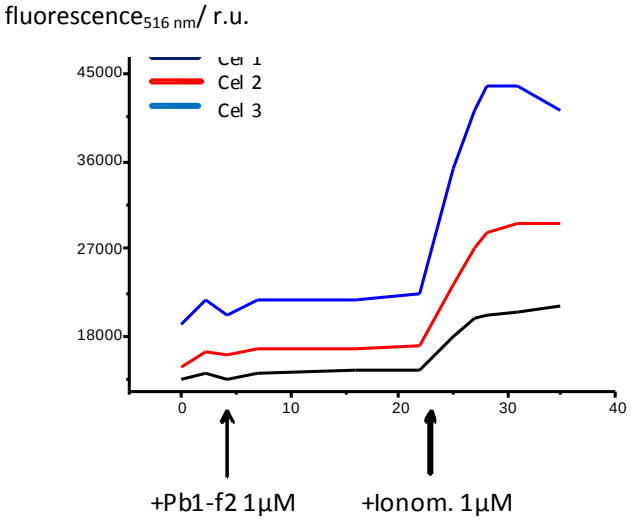

Fig. 44: Fluorescence intensity of Ca2+ sensor Fluo4 in R28 cells. Integral fluorescence signal of 3 exemplary cells recorded before and after addition of 1µM aPB1-F2sf and 1µM Ionomycin to the external medium.

In further experiments the concentration of the added peptide was increased to 10 µM. This treatment resulted in distinct changes in the cytosolic Ca^{2+} concentration. Fig. 45 shows the fluorescence signal from individual cells before and after the addition of 10µM aPB1-F2sf. Before the addition of the peptide the fluorescence signal was low and constant as expected for non-stimulated cells. Some time (ca. 15 min) after adding the viral peptide to the cells, the fluorescence signals from individual cells started to jump from the low resting value to a short lasting elevated level, and then returned to the low level again. In addition also smaller excursion of the fluorescence signal could occur. These spikes must be the result of the aPB1-F2sf activity, since control experiments or recordings with a low peptide concentration were not found to generate these phenomena.

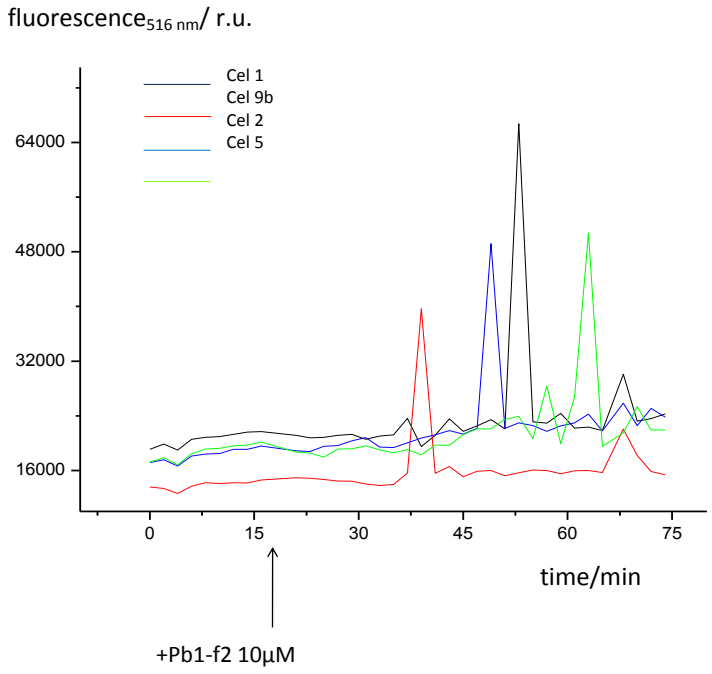

Fig. 45: Increase in the fluorescence of the Ca2+ sensor Fluo-4 in the cytosol of R28 cells after addition of 10µM aPB1-F2sf in the external medium (one measure every 2min).

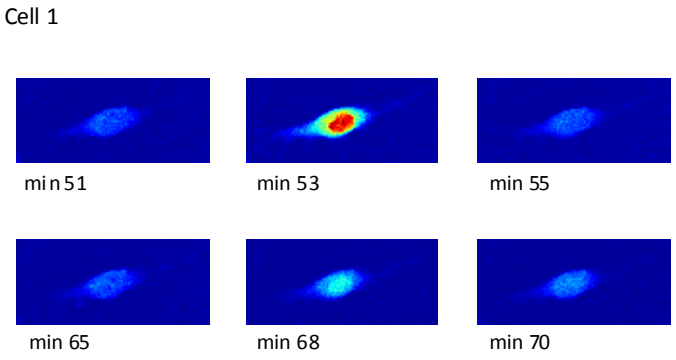

Fig. 46: Two episodes of Fluorescence increase from cell 1, after the addition of 10µM aPB1-F2sf in the external medium. The times indicated along the images correspond to the experimental time given in Fig. 14. The fluorescence signal is elevated in image 2 (min 53) and image 5 (min 68). The Ca^{2+} concentration in the cell is color coded; dark blue color means low and red color high concentration of Ca^{2+}.

The images shown in Fig. 46 were collected during the experiment of Fig. 45. They show the transient increase in fluorescence in cell 1 after addition of aPB1-F2sf to the external solution. Typically the fluorescence increase was not evenly distributed throughout the cell. On the background of an overall elevated Ca^{2+} concentration there was generally a hot spot of even higher fluorescence. This spot is most likely the nucleus meaning that the viral peptide has a strong effect on the Ca^{2+} concentration in the nucleus of cells. An increase of the nucleus internal Ca^{2+} concentration might be an important event since Ca^{2+} signal in the nucleus of other cells was correlated with differential gene activation (Bengtson C.P., et al., 2010).

Model

All together these data demonstrate that aPB1-F2sf is able to affect the conductance of the plasma membrane of mammalian cells. In R28 cells two conductances, which can be distinguished by their difference in kinetics, are increased by the viral peptide. These comprise an instantaneous activating conductance and a slow outward rectifying conductance. It is not yet clear from the data whether the effects on the conductances is direct or indirect. The fact that aPB1-F2sf generates by itself channel conductance in planar lipid bilayers (Henkel et al. 2010) suggests that this could contribute or account for the elevation of the instantaneous activating conductance. The activation of the endogenous outward rectifier must in some way be an indirect consequence of the aPB1-F2sf activity. Since many outward rectifiers are Ca^{2+} sensitive (Bezprozvanny I, et al., 1991) and since PB1-F2 is Ca^{2+} permeable (Henkel et al. 2010) it is in principle possible that the outward rectifier increases as a result of an PB1-F2 mediated increase in cytosolic Ca^{2+} concentration. The present data however do not confirm this hypothesis. At a concentration of 1µM aPB1-F2sf already generates in R28 cells a strong increase in current. Under the same conditions the fluorescence images do not report any increase in cytosolic Ca^{2+} with this concentration. These data suggest that the outward rectifying channels in R28 cells are not activated by an aPB1-F2sf evoked rise in cytosolic Ca^{2+}. This interpretation is further supported by the fact that the response of the currents to 1µM sPB1-F2sf is rapid while the elevation of Ca^{2+} requires minutes to materialize.

While the Ca^{2+} signal, which is stimulated by the viral peptide, may not be important for channel activation, it is nonetheless interesting. The transient character of the Ca^{2+} response is typical for so called Ca^{2+} induced Ca^{2+} oscillations in mammalian cells (Pivovarova N.B. and Andrews S.B., 2010). In this system a small increase in cytosolic Ca^{2+} concentration generally induces together with IP_3, the opening of Ca^{2+} permeable receptor channels in the endoplasmic reticulum. The resulting increase in Ca^{2+} causes an inhibition of the receptor channel; subsequently Ca^{2+} ions are rapidly pumped out of the cytosol into their stores, restoring the physiological Ca^{2+} concentration.

As an alternative reason for the aPB1-F2sf generated increase in currents, we may also think about a direct interaction of the aPB1-F2sf protein with endogenous channels. From mammalian cells it is well known that so called MinK channels are effective modulators of K^+ channels. The MinK channels are like aPB1-F2sf small proteins with a single transmembrane helix. In fact an alignment of aPB1-F2sf with MinK channels shows that the viral protein has some resemblance with MinK proteins.

```
KCNE3           METTNGTETWYESLHAVLKALNATLHSNLLCRPGPGLGPDNQTEERRASLPGRDDNSYMY 60
PB1             MGQEQ-DTPW------ILSTGHISTQKRQDGQQTPKLEHRNSTR-LMGHCQKTMNQVVMP 52
                *   :   .*      :*.: : : :..   :  * *   *.*.   .      ::  *

KCNE3           ILFVMFLFAVTVGSLILGYTRSRKVDKRSDPYHVYIKNRVSMI 103
PB1             KQIVYWKQWLSLRNPILVFLKTRVLKR----WRLFSKHE---- 87
                  :* :   ::: . ** : ::* :.:    :::: *:.
```

Fig. 47: Alignment of aPB1-F2 (PB1) with the MinK protein KCNE3. Identical amino acids are indicated by *. Conserved or similar amino acid exchanges are shown by : or . respectively. Note that many of the positive amino acids in the c-terminal part of KCNE3 have a corresponding basic amino acid in the viral peptide.

Hence aPB1-F2sf might interact in a MinK like manner with endogenous channels and change their activity. This is not unreasonable considering the fact that aPB1-F2sf has a high propensity to associate with endogenous membrane proteins like ANT3 and VDAC1 (Zamarin et al., 2005).

The results described here change the picture of the biological role that Pb1-f2 could have in the infection cycle. The fact that the viral peptide is also affecting the integrity of the plasma membrane implies that the viral molecule can also corrupt cells from outside. This could be relevant in the situation that infected cell or apoptotic cells release the peptide into the extracellular space. In this situation PB1-F2 could insert in the membrane of the surrounding cells. Indeed it has been shown that an addition of PB1-F2 to monocytic cells causes a rapid death of the treated cells (Chen W., et al., 2001; Coleman J.R., 2007). In this way PB1-F2 could for example facilitate the infection of new host cells, act as an infection signal for other viruses, or have a gene regulation effect. New experiments need to be done in order to investigate this hypothesis.

Discussion

aPB1-F2sf

The investigations reported in the result section were expected to contribute to understanding of why many Influenza A viruses are characterized by a strong pathogenic behavior leading to a high mortality of the host cells. In the last years many studies were focused on finding the reason for such a high virulence. Recently it was proposed that the PB1-F2 protein from influenza A may be one of the main factors, which determine the pathogenicity of these viruses.

Our results open the access to a wider field of the effects exerted by PB1-F2 peptides. Up to now, PB1-F2 had been found to be synthesized in infected cells were it inserted in the internal and external mitochondrial membrane (MM) of infected cells, and where it seemed to execute its role as proapoptotic factor. The PB1-F2 protein was found to interact in the mitochondria with ANT3 (in the internal MM) and VDAC1 (in the external MM) with the result that the release of Cytocrome C from the mitochondria to the Cytosol was promoted (Zamarin D. et al., 2005). This release of Cytocrome C was trigging a cascade of events leading to the apoptosis of the host cell. Once in the Cytosol, Cytocrome C interacts indeed also with IP_3, a receptor located in the ER membrane, which induces an increase in cytosolic Ca^{2+}. As a consequence the elevated concentration of Ca^{2+} ions activates caspases proteases. The latter are responsible for the cell apoptosis (Ma X. and Bazan H.E., 2001).

The results reported here overcome the restriction of the action of PB1-F2 solely to the mitochondria. Together with other studies (Chanturiya A.N., et al., 2004; Henklein P., et al., 2005), this work have shown that PB1-F2 is able to generate an elevated conductance in isolated membranes meaning that it could also affect the integrity of membranes other than the mitochondria. So far little was known on the effect of PB1-F2 on other membranes of the host cell. The experiments presented here does not directly describe a possible role of PB1-F2 on cell membranes in the context of the pathogenicity. Nonetheless the present data highlight the propensity of the peptide to insert in membranes including the plasma membrane of cells and generate non-specific channel activity.

We have come to the conclusions mentioned above by three different approaches: studying PB1-F2 single channel activity in artificial lipid bilayer (Fig. 33), measuring its macro currents in mammalian cells (Fig. 35, Fig. 42), and testing its induced cytosolic calcium increase (Fig. 45).

Single-channel characterization of aPB1-F2sf in artificial lipid bilayer

Single-channel recordings of aPB1-F1sf in lipid membranes enabled the observation of a phenomenon which was observed also with three other PB1-F2 peptides from different Influenza A viral strains (Henkel et al., 2010). A detailed investigation of the aPB1-F2sf protein shows that it generates the same single channel fluctuations as other PB1-F2 proteins from other virus sources (Fig. 34). This includes more than one conductance level at different voltages, or even in the same opening event (Fig. 33b).Channel formation by PB1-F2 may result from the interaction of a variable number of subunits: the higher is the number of subunits, the higher will be the conductance. We can speculate that a subunit insertion or deletion event could occur even when the channel is in a conductive state.

Furthermore, as in the case of the other PB1-F2 proteins, also aPB1-F2sf generated higher conductances at extreme potentials (Fig. 33a). The finding of such a high number of sublevels may lead to an understanding of the underlying mechanism: it seems that at extreme voltages the interaction of a higher number of subunits is promoted. This hypothesis might be confirmed also by the measurements done with another PB1-F2 peptide, encoded by the Puerto Rico Influenza virus: the mean current, plotted against the membrane potential, increases at extreme voltages, (Henkel et al, 2009).

Considered the similar characteristics of aPB1-F2sf with PB1-F2 peptides encoded by other viral strains, we assume that also the peptide derived from swine Flu virus could have the same behavior. This result is of great interest in the view of spontaneous mutations that can modify the genetic sequence of the H1N1 swine Flu virus. It means that a future mutation in the swine Flu will most likely generate a gene which will code for a full length PB1-F2 proteins. The gene product will be able to function as other PB1-F2 proteins as channel forming peptide in infected cells.

On the basis of the demonstrated propensity of PB1-F2 to insert in membranes, we went on exploring its behavior in mammalian cell membranes.

PB1-F2 generates an elevated conductance in mammalian cells plasma membrane

The aforementioned data imply that the viral peptide is able to generate channel fluctuations in planar lipid bilayers. This implies that the peptide does not necessarily only interact with mitochondrial membranes; it could in principle corrupt the integrity of any cellular membrane. In this context it is also interesting to examine the effect of the viral peptide on the plasma membrane of cells. This information can be important for the full understanding of its role during the viral infection.

The monitoring of plasma membrane currents of R28 cells shows that an addition of aPB1-F2sf to the external medium causes a quasi immediate increase in membrane conductance in these cells. This effect is not cell specific because it is also observed in HEK 293 cells implying that the peptide generates a generic increase in membrane conductance in mammalian cells.

The aPB1-F2sf induced increase in membrane conductance in R28 cells can be decomposed into two different kinetic components: an elevation of an instantaneous current and of the endogenous time dependent outward rectifier. Different mechanisms could be at the basis of this phenomenon. A reasonable explanation for the increase in instantaneous current is that the PB1-F2 peptide inserts into the plasma membrane and generates already by itself a non selective conductance. The effect on the time dependent conductance is more difficult to explain because in this case the viral peptide causes an increase in an endogenous current; hence the mode of action must be indirect. This concept is supported by the findings in Fig. 40 which show that this slow component has the same curve shape as the intrinsic channel of the mammalian cell has. The effect of aPB1-F2sf is just an up scaling of the activity of this intrinsic channel. This finding leads to the assumption that aPB1-F2sf exerts an indirect effect on an intrinsic channel in addition to the direct effect which becomes obvious in the Instantaneous current.

One possibility is that the outward-rectifying K^+ channel is Ca^{2+} dependent, and that aPB1-F2sf generated increase in cytosolic Ca^{2+} modifies its activity. This hypothesis is not unreasonable since the PB1-F2 proteins were found to generate channels pores with Ca^{2+} permeability.

Nevertheless, as long as the putative Ca^{2+} influx has not been shown, alternative mechanisms should be considered. Such a mechanism for the activation of the outward rectifier by aPB1-F2sf could be related to the structure of the peptide, which shares some similarity to the MinK subunits. These single transmembrane α-helices are known to activate or modulate the activity of K^+ channels (Barhanin J. et al., 1996; Sanguinetti M.C., et al., 1996), altering in some cases their gating properties, or even their sensitivity to blockers.

Currently it is not yet possible to decide between the two hypotheses. It is for example not yet clear whether the outward rectifier in R28 cells is Ca^{2+} sensitive. This point still needs to be examined. Nonetheless the measurements of the cytosolic Ca^{2+} concentration are already providing some insight into

the action of PB1-F2 peptides in R28 cells. The microfluorimetric data show that that aPB1-F2sf indeed causes a transient increase of Cytosolic Ca^{2+}. This is expected from the fact that the PB1-F2 peptide generates Ca^{2+} permeable channels. The rise in Ca^{2+} however requires a aPB1-F2sf concentration of 10µM, while the increase in outward rectifier conductance is achieved already with 100nM peptide.

This together with the observation that the Ca^{2+} signal occurs only after minutes of a lag time while the conductance reacts quasi immediately strongly suggest that PB1-F2 is not stimulating the outward rectifier via Ca^{2+}.

Whereas the PB1-F2 generated rise in cytosolic Ca^{2+} is probably not important for the regulation of currents, it is by itself an interesting phenomenon. The most important observation is that the viral peptide causes a transient and repetitive rise in the cytosolic Ca^{2+} concentration. This phenomenon could be interpreted as the well known *Ca^{2+} induced Ca^{2+} release* in mammalian cells. The process is generally induced by a small leak of Ca^{2+} at the plasma membrane. In the present case, the initial Ca^{2+} increase could be generated by the PB1-F2 channels in the cell membrane. The small rise in cytosolic Ca^{2+} is then amplified by a concerted action of IP_3, which activate a receptor channel in the endoplasmic reticulum, thus causing a massive release of Ca^{2+} from internal stores. High concentrations of Ca^{2+} are auto inhibiting the receptor channel, and Ca^{2+} is pumped back into the stores before the next wave of release is initiated.

On the background of the immense importance of cytosolic Ca^{2+} as a second messenger in cells, it is reasonable to believe that a PB1-F2 generated Ca^{2+} signal could result in a large number of cellular responses. This includes for example the possible trigging of the apoptotic signal in infected cells. The fact that Ca^{2+} waves are propagated even into the cell nucleus suggests that PB1-F2 could even have effects on gene regulation.

Possible role of PB1-F2 in Influenza A infection cycle

The main information from the present study is that PB1-F2 does not only corrupt the membrane integrity of mitochondria. It can also affect cells from the external side by altering the conductance of the plasma membrane and by affecting Ca^{2+}-dependent signal transduction mechanisms in cells. In this context it is worth mentioning that already the first publication in which PB1-F2 has been initially described reports that the viral peptide is able to kill mammalian cell when added at low concentrations to the external medium. Hence it is reasonable to speculate that the peptide, which is synthesized in infected cells is either sequestered into the external medium or released after cell death (Chen W., et al., 2001). From there it can attack cells in the surrounding of the primary infected cells. This event could induce cells apoptosis and increase the lung attack by *Streptococcus pneumoniae*, as described for infection from PB1-F2 encoding Influenza A viruses (McAuley J.L., et al., 2007).

New experiments will be done in order to investigate on these hypothesis.

Conclusions

During my PhD I've been working in order to elucidate the characteristics of two different viral channels. The study of viruses is of growing interest because of the many possible usage of their knowledge for biological and medical applications. We have seen for example that phylogenetic studies on viral genome and proteins is useful for the description of cell origins and the construction of evolutionary theories, providing knowledge not only with respect to viruses, but concerning also other different biological systems.

Viral diseases have a strong impact, as infection factors, on the control of a population, and can be considered as important biological agents that establish an equilibrium between them and the infected organisms. On this view, an important application of the study of viral proteins is the design of new, more specific and more effective antiviral drugs. In particular, ion channels can be considered as possible target for this purpose, because of the possibility to interact and block their electrical activity. Ion channels blockers, such as Amantadine or Rimantadine, are already used as antiviral molecules; however, their usage can be denied by an unspecific action on other ion channels, and therefore by the related complications. From here, the interest in the research of specific viral channels blockers.

The research of proteins related with a higher viral pathogenic behavior is of great interest in the understanding of infection mechanisms and development of antiviral molecules. Single transmembrane peptides with characteristics similar to PB1-F2 are encoded also by other viruses (like HIV-1 Vpu), and the description of its properties can elucidate the behavior of a multitude of viruses.

The properties described for viroporins can then be applied to the study of more complexes prokaryotic or eukaryotic ion channels. As previously discussed, viral peptides represents the minimal functional module needed for a functional protein, and viral channels such as Kcv can be considered as models useful for the understanding of potassium channels properties. We prospect in the future that the description of PBCV-1 Kcv gating mechanisms will foster the understanding of inherent properties relatively to the pore region of potassium channels.

We are experimenting in our laboratory the possibility to take advantage of the knowledge on Kcv gating properties in order to build a biosensor chimera: hybridating the viral channel with other modules, sensitive to changes of environmental factors, we expect to induce a conformational change of the channel structure, and that such a modification can modulate a gating mechanism, and therefore the biophysical properties of the chimerical channel. A change in the surrounding conditions can be then transducted by measuring the electrical signal.

New projects are focalized on testing electrophysiological and sensitivity characteristics of Kcv channels hybridated with a Calmodulin domain, sensitive to free Ca^{2+} concentration, or with the voltage sensor domain from other potassium channels.

References

Neher E. and Sakmann B. (1976) Single-channel currents recorded from membrane of denervated frog muscle fibres. Nature. 1976 Apr 29;260(5554):799-802.

Neher E., Sakmann B. and Steinbach J.H. (1978) The extracellular patch clamp: a method for resolving currents through individual open channels in biological membranes. Pflugers Arch. 1978 Jul 18;375(2):219-28.

Cannon S.C. (2010) Voltage-sensor mutations in channelopathies of skeletal muscle. J Physiol. 2010 Jun 1;588(Pt 11):1887-95. Epub 2010 Feb 15. Review.

Armstrong C.M. and Bezanilla F. (1973) Currents related to movement of the gating particles of the sodium channels. Nature. 1973 Apr 13;242(5398):459-61.

Perozo E., Cortes D.M., Cuello L.G (1999) Structural rearrangements underlying K+-channel activation gating. Science. 1999 Jul 2;285(5424):73-8.

Blunck R, Cordero-Morales JF, Cuello LG, Perozo E, Bezanilla F. (2006) Detection of the opening of the bundle crossing in KcsA with fluorescence lifetime spectroscopy reveals the existence of two gates for ion conduction. J Gen Physiol. 2006 Nov;128(5):569-81. Epub 2006 Oct 16.

Cordero-Morales JF, Cuello LG, Perozo E. (2006) Voltage-dependent gating at the KcsA selectivity filter. Nat Struct Mol Biol. 2006 Apr;13(4):319-22. Epub 2006 Mar 12.

Hagiwara S, Miyazaki S, Krasne S, Ciani S. (1977) Anomalous permeabilities of the egg cell membrane of a starfish in K+-Tl+ mixtures. J Gen Physiol. 1977 Sep;70(3):269-81.

Lockless S.W., Zhou M., MacKinnon R (2007) Structural and thermodynamic properties of selective ion binding in a K+ channel. PLoS Biol. 2007 May;5(5):e121.

Zheng and Sigworth (1997) Selectivity changes during activation of mutant Shaker potassium channels. J Gen Physiol. 1997 Aug;110(2):101-17.

Zheng and Sigworth (1998) Intermediate conductances during deactivation of heteromultimeric Shaker potassium channels. J Gen Physiol. 1998 Oct;112(4):457-74.

Lustig A, Levine AJ. (1992) One hundred years of virology. J Virol. 1992 Aug;66(8):4629-31.

L.P. Villarreal and V.R. DeFilippis (2000) A hypothesis for DNA viruses as the origin of eukaryotic replication proteins. J Virol. 2000 Aug;74(15):7079-84.

J.M. Claverie and C. Abergel (2010) Mimivirus: the emerging paradox of quasi-autonomous viruses. Trends Genet. 2010 Oct;26(10):431-7. Epub 2010 Aug 7.

Wozniak AL, Griffin S, Rowlands D, Harris M, Yi M, Lemon SM, Weinman SA. (2010) Intracellular proton conductance of the hepatitis C virus p7 protein and its contribution to infectious virus production. PLoS Pathog. 2010 Sep 2;6(9):e1001087.

Hsu K, Han J, Shinlapawittayatorn K, Deschenes I, Marbán E. (2010) Membrane potential depolarization as a triggering mechanism for Vpu-mediated HIV-1 release. Biophys J. 2010 Sep 22;99(6):1718-25.

Van Etten JL, Lane LC, Meints RH. (1991) Viruses and viruslike particles of eukaryotic algae. Microbiol Rev. 1991 Dec;55(4):586-620.

Van Etten JL, Meints RH. (1999) Giant viruses infecting algae. Annu Rev Microbiol. 1999;53:447-94.

Mehmel M, Rothermel M, Meckel T, Van Etten JL, Moroni A, Thiel G. (2003) Possible function for virus encoded K+ channel Kcv in the replication of chlorella virus PBCV-1. FEBS Lett. 2003 Sep 18;552(1):7-11.

Plugge, B., S. Gazzarrini, M. Nelson, R. Cerana, J.L. Van Etten, C. Derst, D. DiFrancesco, A. Moroni, and G. Thiel. 2000. A potassium channel protein encoded by chlorella virus PBCV-1. Science. 287:1641–1644.

Gazzarrini, S., J.L. Etten, D. DiFrancesco, G. Thiel, and A. Moroni. 2002. Voltage-dependence of virus-

encoded miniature K+ channel Kcv. J. Membr. Biol. 187:15–25.

Gazzarrini, S., A. Abenavoli, D. Gradmann, G. Thiel, and A. Moroni. 2006. Electrokinetics of miniature K+ channel: open-state V sensitivity and inhibition by K+ driving force. J. Membr. Biol. 214:9–17.

Hertel B, Tayefeh S, Mehmel M, Kast SM, Van Etten J, Moroni A, Thiel G. (2006) Elongation of outer transmembrane domain alters function of miniature K+ channel Kcv. J Membr Biol. 2006 Mar;210(1):21-9. Epub 2006 May 17.

Syeda R, Holden MA, Hwang WL, Bayley H (2008) Screening blockers against a potassium channel with a droplet interface bilayer array. J Am Chem Soc 130: 15543–15548.

Pinto LH, Lamb RA (2007) Controlling influenza virus replication by inhibiting its proton channel. Mol Biosyst 3: 18–23.

Wagner M, Riepe KG, Eberhardt E, Volk T.(2010) Open channel block of the fast transient outward K+ current by primaquine and chloroquine in rat left ventricular cardiomyocytes. Eur J Pharmacol. 2010 Nov 25;647(1-3):13-20. Epub 2010 Aug 31.

Pagliuca, C., T.A. Goetze, R. Wagner, G. Thiel, A. Moroni, and D. Parcej. 2007. Molecular properties of Kcv, a virus encoded K+ channel. Biochemistry. 46:1079–1090.

Shim, J.W., M. Yang, and L.Q. Gu. 2007. In vitro synthesis, tetramerization and single channel characterization of virus-encoded potassium channel Kcv. FEBS Lett. 581:1027–1034.

Kuo, A., J.M. Gulbis, J.F. Antcliff, T. Rahman, E.D. Lowe, J. Zimmer, J. Cuthbertson, F.M. Ashcroft, T. Ezaki, and D.A. Doyle. 2003. Crystal structure of the potassium channel KirBac1.1 in the closed state. Science. 300:1922–1926.

Tayefeh, S., T. Kloss, G. Thiel, B. Hertel, A. Moroni, and S.M. Kast. 2007. Molecular dynamics simulation of the cytosolic mouth in Kcv-type potassium channels. Biochemistry. 46:4826–4839.

Moroni, A., C. Viscomi, V. Sangiorgio, C. Pagliuca, T. Meckel, F. Horvath, S. Gazzarrini, P. Valbuzzi, J.L. Van Etten, D. DiFrancesco, and G. Thiel. 2002. The short N-terminus is required for functional expression of the virus-encoded miniature K(+) channel Kcv. FEBS Lett. 530:65–69.

Clarke OB, Caputo AT, Hill AP, Vandenberg JI, Smith BJ, Gulbis JM. (2010) Domain reorientation and rotation of an intracellular assembly regulate conduction in Kir potassium channels. Cell. 2010 Jun 11;141(6):1018-29.

Y. Zhou, J. H. Morais-Cabral, A. Kaufman, R. MacKinnon (2001) Chemistry of ion coordination and hydration revealed by a K+ channel–Fab complex at 2.0 resolution", Nature 2001, 414, 43 – 48.

Cuello LG, Jogini V, Cortes DM, Perozo E. (2010) Structural mechanism of C-type inactivation in K(+) channels. Nature. 2010 Jul 8;466(7303):203-8.

Rotem D, Mason A, Bayley H. (2010) Inactivation of the KcsA potassium channel explored with heterotetramers. J Gen Physiol. 2010 Jan;135(1):29-42.

Cordero-Morales JF, Jogini V, Lewis A, Vásquez V, Cortes DM, Roux B, Perozo E. (2007) Molecular driving forces determining potassium channel slow inactivation. Nat Struct Mol Biol. 2007 Nov;14(11):1062-9. Epub 2007 Oct 7.

Fitzhugh, R. 1983. Statistical properties of the asymmetric random telegraph signal, with applications to single-channel analysis. Math. Biosci. 64:75–89.

Colquhoun D, Hawkes AG. (1990) Stochastic properties of ion channel openings and bursts in a membrane patch that contains two channels: evidence concerning the number of channels present when a record containing only single openings is observed. Proc R Soc Lond B Biol Sci. 1990 Jun 22;240(1299):453-77.

Schroeder, I., and U.P. Hansen. 2007. Saturation and microsecond gating of current indicate depletion-induced instability of the MaxiK selectivity filter. J. Gen. Physiol. 130:83–97.

Y. Zhou, R. MacKinnon, (2003) “The occupancy of ions in the K+ selectivity filter: Charge balance and coupling of ion binding to a protein conformational change underlie high conduction rates”: J. Mol. Biol. 2003, 333, 965 – 975.

Schroeder, I., and U.P. Hansen. 2006. Strengths and limits of Beta distributions as a means of reconstructing the true single-channel current in patch clamp time series with fast gating. J. Membr. Biol. 210:199–212.

Alessandra Abenavoli,1 Mattia Lorenzo DiFrancesco,1 Indra Schroeder,2 Svetlana Epimashko,1 Sabrina Gazzarrini,1 Ulf Peter Hansen,2 Gerhard Thiel,3 and Anna Moroni1 (2009) Fast and slow gating are inherent properties of the pore module of the K+ channel Kcv J Gen Physiol. 2009 Sep;134(3):219-29.

Dunlop J, Jones PC, Finbow ME. (1995) Membrane insertion and assembly of ductin: a polytopic channel with dual orientations. EMBO J. 1995 Aug 1;14(15):3609-16.

Marques EJ, Carneiro CM, Silva AS, Krasilnikov OV. (2004) Does VDAC insert into membranes in random orientation? Biochim Biophys Acta. 2004 Feb 10;1661(1):68-77.

Dart C. (2010) Lipid microdomains and the regulation of ion channel function. J Physiol. 2010 Sep 1;588(Pt 17):3169-78. Epub 2010 Jun 2.

Galan C, Woodard GE, Dionisio N, Salido GM, Rosado JA. (2010) Lipid rafts modulate the activation but not the maintenance of store-operated Ca(2+) entry. Biochim Biophys Acta. 2010 Sep;1803(9):1083-93.

Beveridge W.I. (1991) The chronicle of influenza epidemics. Hist Philos Life Sci. 1991;13(2):223-34.

Johnson N.P. and Muller J. (2002) Updating the accounts: global mortality of the 1918-1920 "Spanish" influenza pandemic. Bull Hist Med. 2002 Spring;76(1):105-15.

Sethi S (2002) Bacterial pneumonia. Managing a deadly complication of inXuenza in older adults with

comorbid disease. Geriatrics 57:56–61

Zamarin D, Ortigoza MB, Palese P (2006) InXuenza A virus PB1-F2 protein contributes to viral pathogenesis in mice. J Virol 80:7976–7983

McAuley JL, Hornung F, Boyd KL, Smith AM, McKeon R, et al. (2007) Expression of the 1918 influenza A virus PB1-F2 enhances the pathogenesis of viral and secondary bacterial pueumonia. Cell Host & Microbe 2: 240–249.

Chevalier C, Al Bazzal A, Vidic J, Fevier V, Bourdieu C, et al. (2010) PB-1F2 influenza A virus protein adopts a beta-sheet conformation and forms amyloid fibres in a membrane environment. J Biol Chem (in press).

Zell R, Krumbholz A, Wutzler P (2006) InXuenza A virus PB1-F2 gene. Emerg Infect Dis 12:1607–1608 (author reply 1608–1609)

Zell R, Krumbholz A, Eitner A, Krieg R, Halbhuber K-J, et al. (2007) Prevalance of PB1-F2 of influenza A viruses. J Gen Virol 88: 536–546.

Conenello GM, Zamarin D, Perrone LA, Tumpey T, Palese P (2007) A single mutation in the PB1-F2 of H5N1 (HK/97) and 1918 influenza A viruses contribute to increased virulence. Plos Pathogens 3: 1414–1421.

Hai R, Schmolke M, Varga ZT, Manicassamy B, Wang TT, Belser JA, Pearce MB, García-Sastre A, Tumpey TM, Palese P (2010) PB1-F2 expression by the 2009 pandemic H1N1 influenza virus has minimal impact on virulence in animal models. J Virol. 2010 May;84(9):4442-50.

Henkel M, Mitzner D, Henklein P, Meyer-Almes FJ, Moroni A, Difrancesco ML, Henkes LM, Kreim M, Kast SM, Schubert U, Thiel G. (2010) The proapoptotic influenza A virus protein PB1-F2 forms a nonselective ion channel. PLoS One. 2010 Jun 15;5(6):e11112.

Chanturiya AN, Basanez G, Schubert U, Henklein P, Yewdell JW, Zimmerberg J (2004) PB1-F2, an inXuenza A virus-encoded proapoptotic mitochondrial protein, creates variably sized pores in planar lipid

membranes. J Virol 78:6304–6312

Mauerer UR, Boulpaep EL, Segal AS. (1998) Regulation of an inwardly rectifying ATP-sensitive K+ channel in the basolateral membrane of renal proximal tubule. J Gen Physiol. 1998 Jan;111(1):161-80.

Pian P, Bucchi A, Robinson RB, Siegelbaum SA. (2006) Regulation of gating and rundown of HCN hyperpolarization-activated channels by exogenous and endogenous PIP2. J Gen Physiol. 2006 Nov;128(5):593-604.

Chen W, Calvo PA, Malide D, Gibbs J, Schubert U, et al. (2001) A novel influenza A virus mitochondrial protein that induces cell death. Nat Med 7: 1306–1312.

Gibbs JS, Malide D, Hornung F, Bennink JR, Yewdell JW (2003) The inXuenza A virus PB1-F2 protein targets the inner mitochondrial membrane via a predicted basic amphipathic helix that disrupts mitochondrial function. J Virol 77:7214–7224

Barhanin J, Lesage F, Guillemare E, Fink M, Lazdunski M, Romey G. (1996) K(V)LQT1 and lsK (minK) proteins associate to form the I(Ks) cardiac potassium current. Nature. 1996 Nov 7;384(6604):78-80.

Sanguinetti MC, Curran ME, Zou A, Shen J, Spector PS, Atkinson DL, Keating MT. (1996) Coassembly of K(V)LQT1 and minK (IsK) proteins to form cardiac I(Ks) potassium channel. Nature. 1996 Nov 7;384(6604):80-3.

Zamarin D, Garcia-Sastre A, Xiao X, Wang R, Palese P (2005) InXuenza virus PB1-F2 protein induces cell death through mitochondrial ANT3 and VDAC1. PLoS Pathog 1:e4

Smaili S, Hirata H, Ureshino R, Monteforte PT, Morales AP, Muler ML, Terashima J, Oseki K, Rosenstock TR, Lopes GS, Bincoletto C. (2009) Calcium and cell death signaling in neurodegeneration and aging. An Acad Bras Cienc. 2009 Sep;81(3):467-75.

Bengtson CP, Freitag HE, Weislogel JM, Bading H. (2010) Nuclear Calcium Sensors Reveal that Repetition

of Trains of Synaptic Stimuli Boosts Nuclear Calcium Signaling in CA1 Pyramidal Neurons. Biophys J. 2010 Dec 15;99(12):4066-77.

Bezprozvanny I, Watras J, Ehrlich BE. (1991) Bell-shaped calcium-response curves of Ins(1,4,5)P3- and calcium-gated channels from endoplasmic reticulum of cerebellum. Nature. 1991 Jun 27;351(6329):751-4.

Pivovarova NB, Andrews SB. (2010) Calcium-dependent mitochondrial function and dysfunction in neurons. FEBS J. 2010 Sep;277(18):3622-36. doi: 10.1111/j.1742-4658.2010.07754.x.

Coleman JR (2007) The PB1-F2 protein of inXuenza A virus: increasing pathogenicity by disrupting alveolar macrophages. Virol J 4:9

Dedicato a…

alla Nostra piccola grande Marika,

ad Attila,

al caro Nonno Enzo,

alla mia Famiglia,

ai Compagni di Università,

ai Compagni di Vita,

a Noi,

al passato,

al presente…

al futuro!!!